Experimentelle Methoden der Teilchenphysik

Sommersemester 2011/2012

Albert-Ludwigs-Universität Freiburg

Prof. Markus Schumacher

Physikalisches Institut, Westbau, 2. OG Raum 008

Telefon 07621 203 7612

E-Mail: Markus.Schumacher@physik.uni-freiburg.de

Kapitel 7: Kalorimeter/Schauerzähler

http://terascale.physik.uni-freiburg.de/lehre/Sommersemester%202012

Erinnerung: WW mit Materie für Elektronenund Photonen

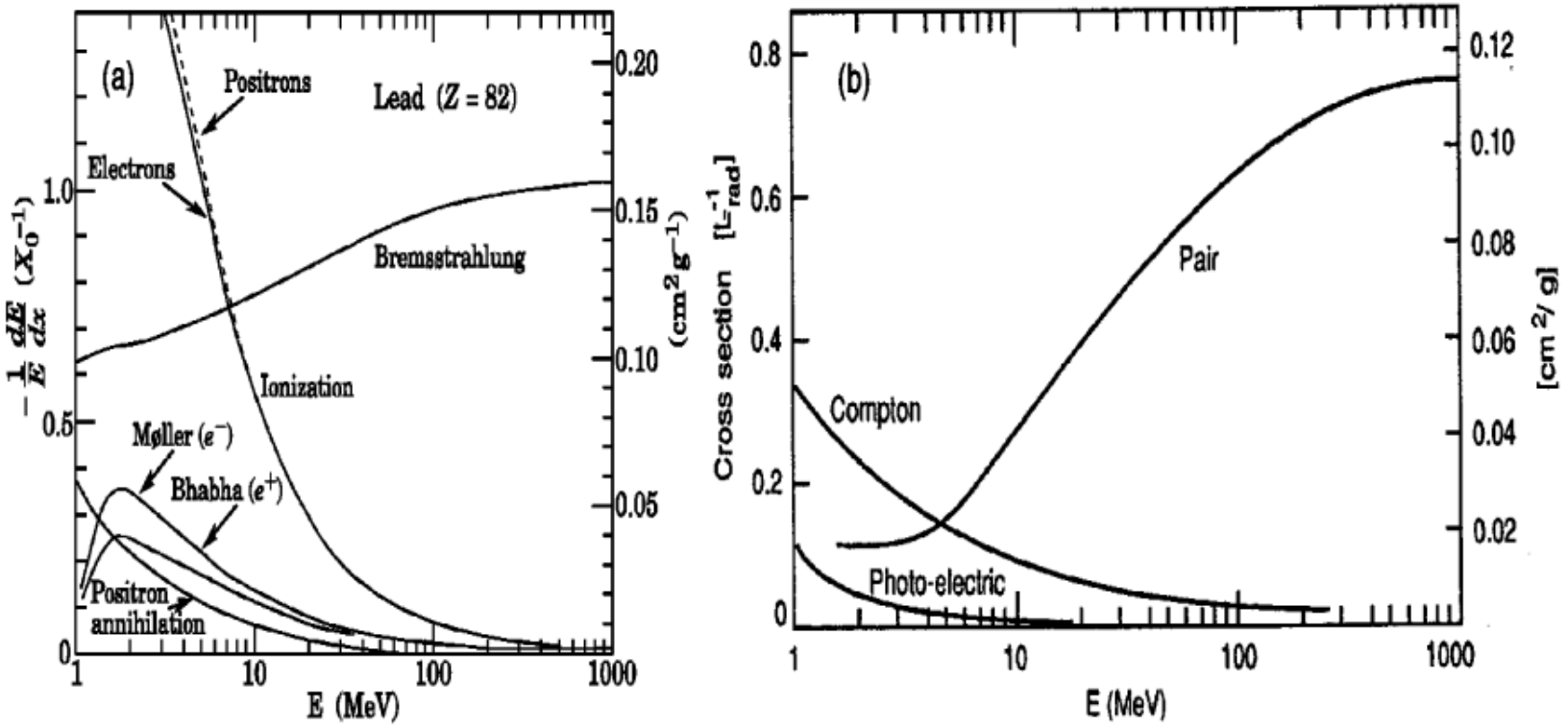

FIG. 1. (a) Fractional energy lost in lead by electrons and positrons as a function of energy (Particle Data Group, 2002). (b) Photon interaction cross section in lead as a function of energy (Fabjan, 1987).

Elektromagnetischer Schauer

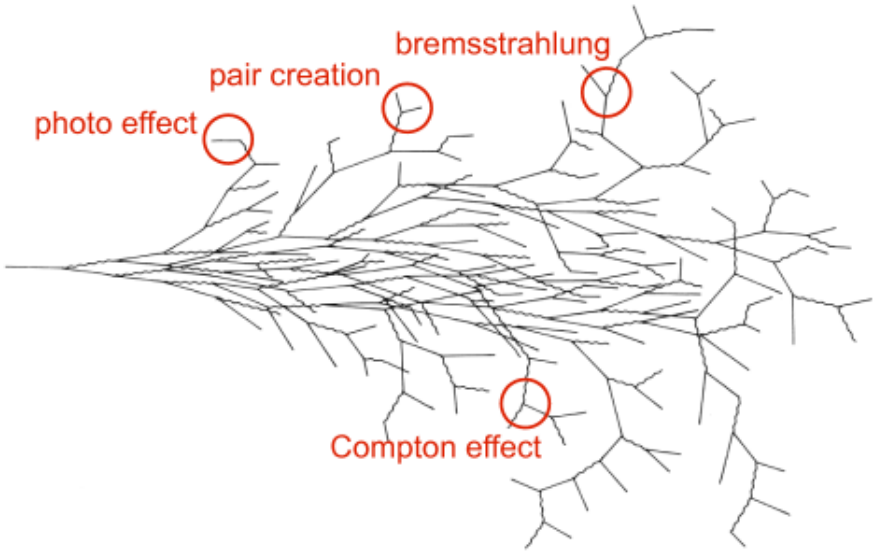

Fig. 7.20. Schematic representation of an electromagnetic cascade. The wavy lines are photons and the solid lines electrons or positrons.

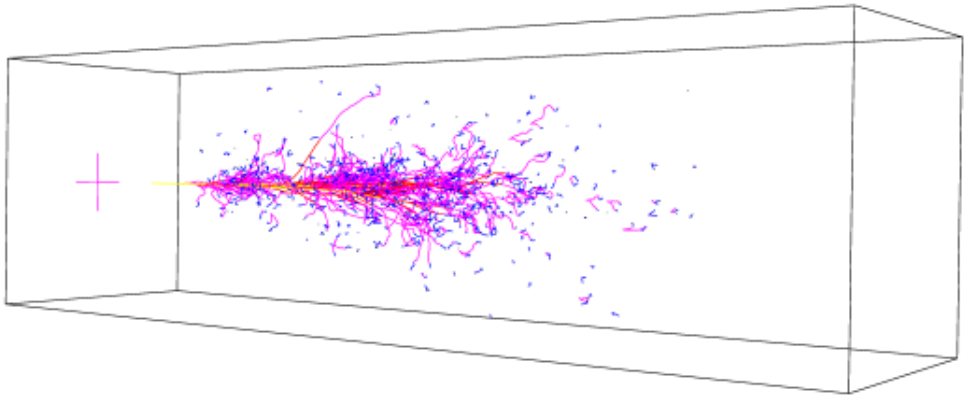

Elektromagnetisches Schauerprofil

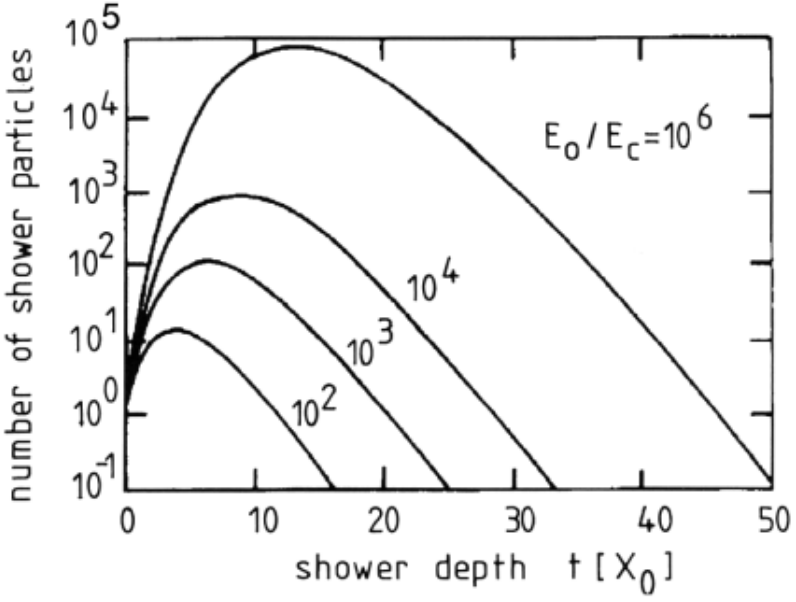

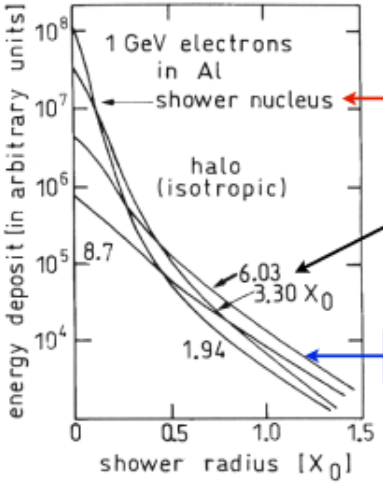

dominated by $\Theta_{brems}=p_e/m_e$

longitudinal depth

dominated multiple scattering

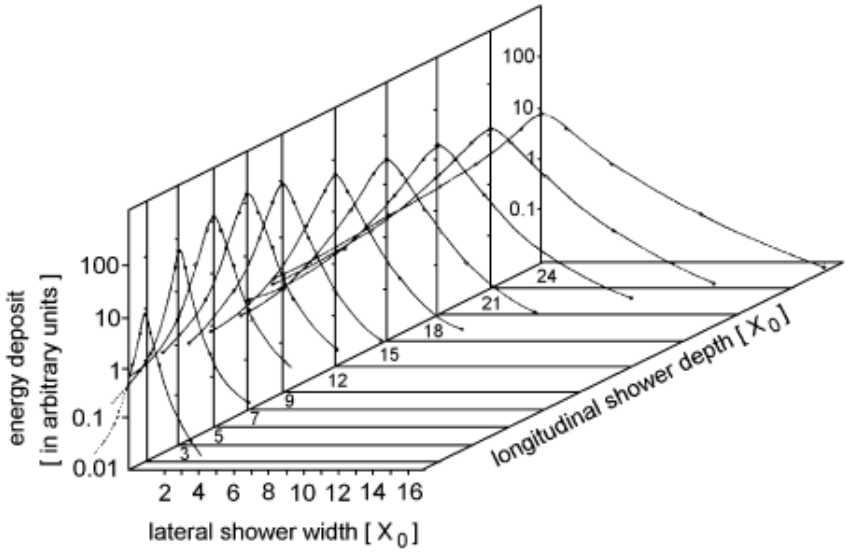

Elektromagnetisches Schauerprofil: Vgl. Photon und Elektron

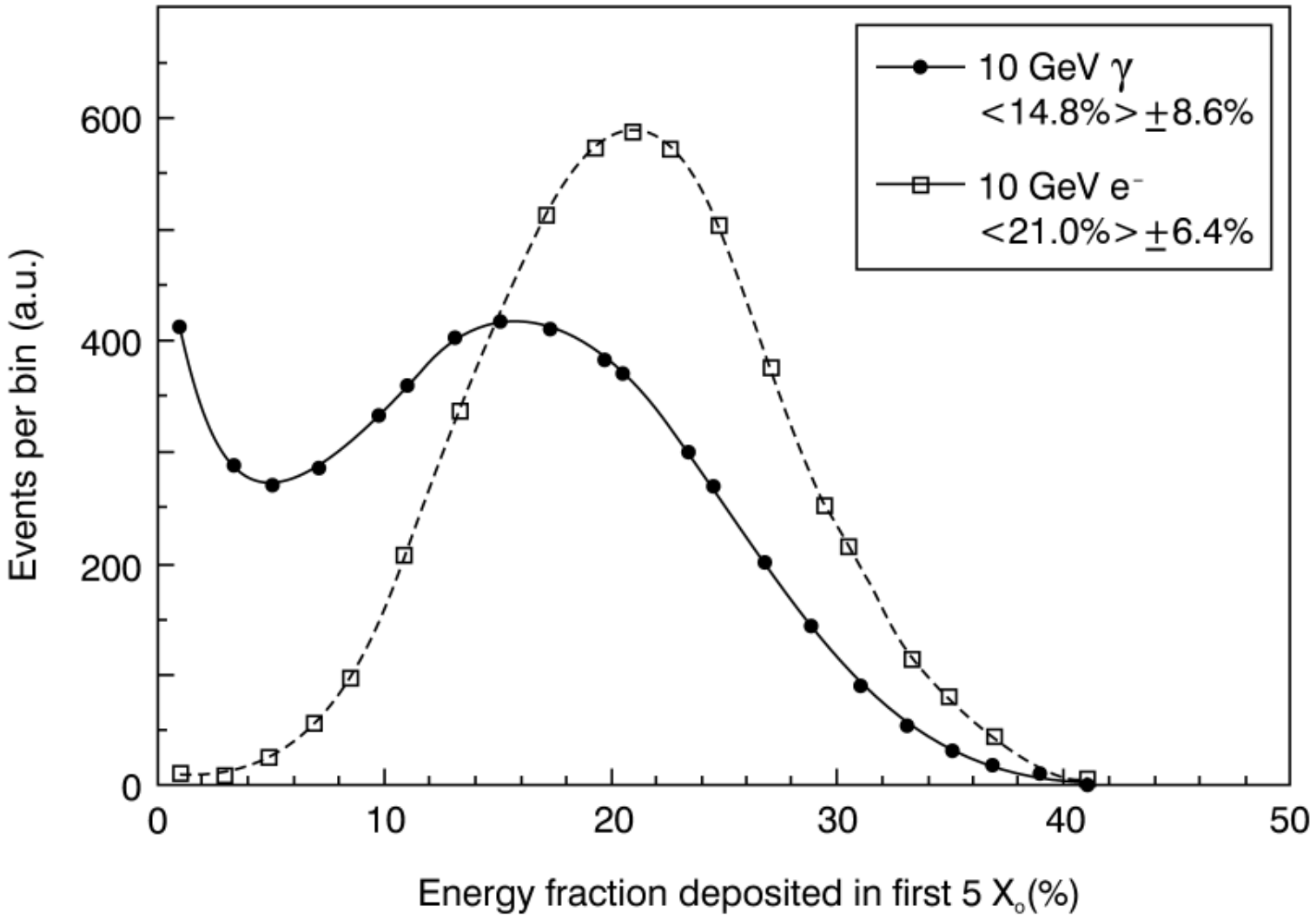

Elektromagnetisches Schauerprofil: Materialabhängigkeit

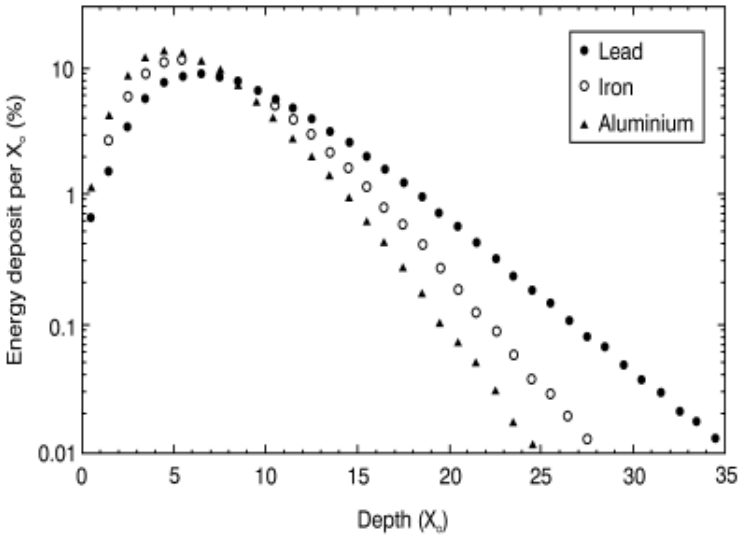

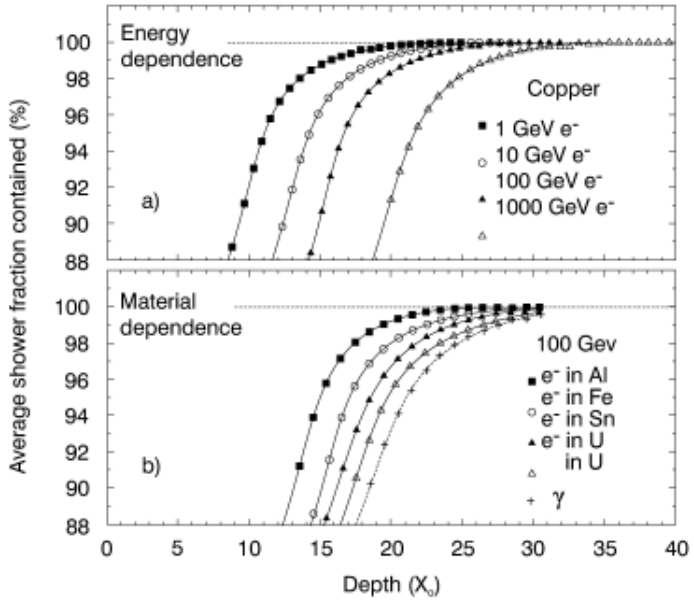

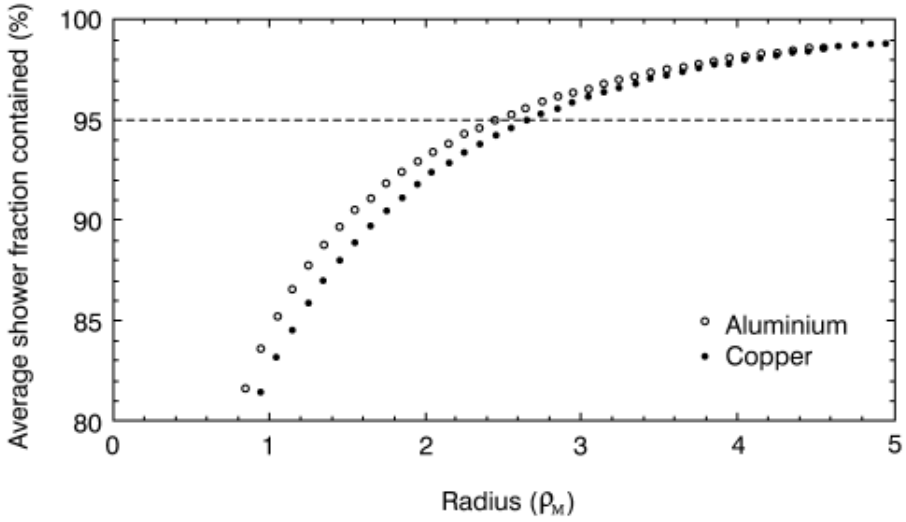

Elektromagnetisches Schauerprofil: Energie pro Teilchen

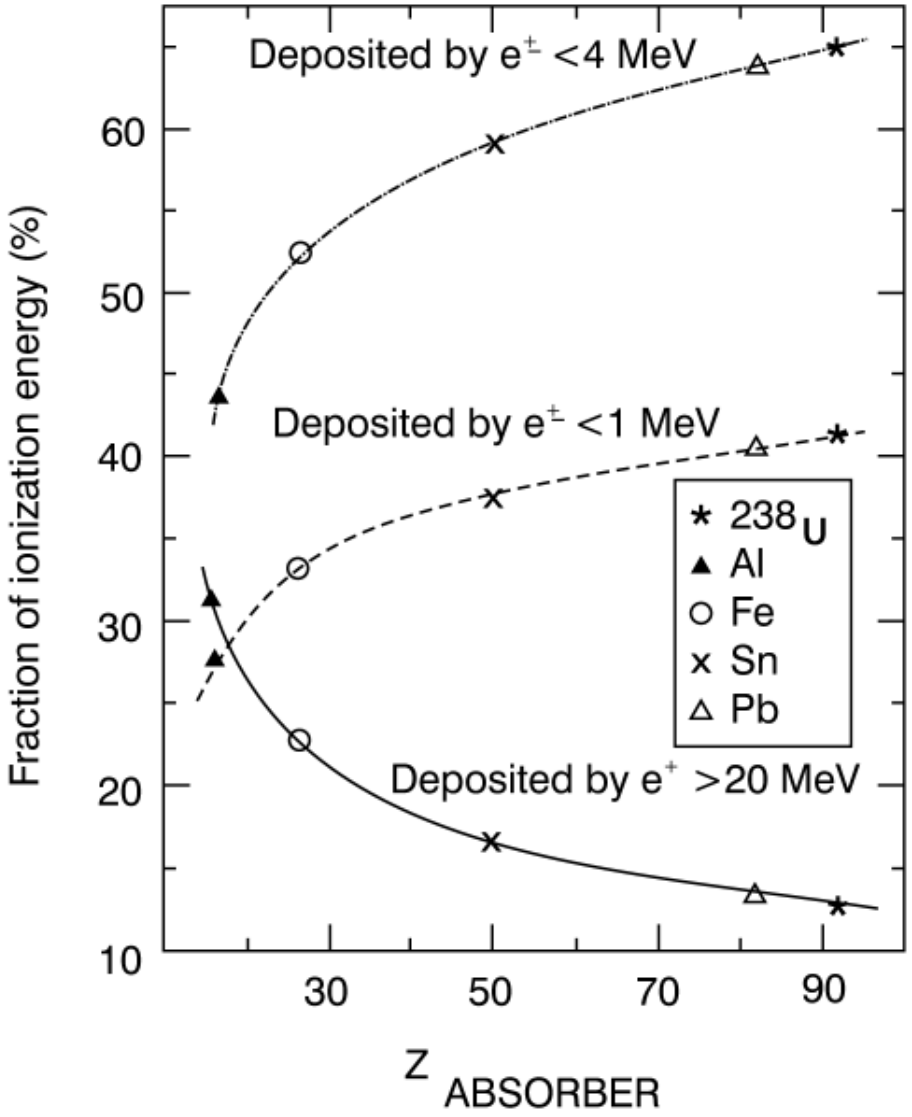

Energieauflösung: ein Beispiel

Energy resolution: General considerations

Intrinsic fluctuations

- Track length T: Total length of all charged particle tracks within a calorimeter
- Total detectable track length:

$$z = 4.58 \frac{Z}{A} \frac{E_{min}}{E_c}$$

$$F(z) = e^z \left[1 + z \ln(z/1.526)\right]$$

$$T = F(z) \frac{E_0}{E_c}$$

- Number of energy depositions above minimum detectable energy E_{min} :

$$N_{max} = E_0 / E_{min}$$

- Intrinsic resolution:

$$(\sigma_E/E)_{intrinsic} \sim \sigma_{N_{max}}/N_{max} = 1/\sqrt{N_{max}} \propto 1/\sqrt{E_0}$$

- Illustrative example: Pb-glass

$$E_{min} \simeq 0.7 MeV \text{ for } E_0 = 1 GeV$$

$$N_{max} = 1000/0.7 = 1500$$

⇒ Resolution: few percent!

Intrinsic sampling fluctuations

- In a sampling calorimeter, one determines not the total track length T but only a fraction of it depending on the thickness of passive and active absorber plates
- Number of crossings:
- Sampling resolution:

$$N_x = \frac{T_d}{d} = F(z) \frac{E_0}{E_c d}$$

$$(\sigma_E/E)_{sampling} \sim \sigma_{N_x}/N_x = 1/\sqrt{N_x}$$

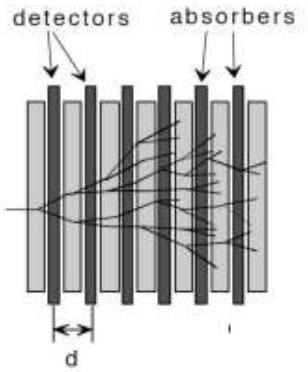

Energieauflösung: ein Beispiel

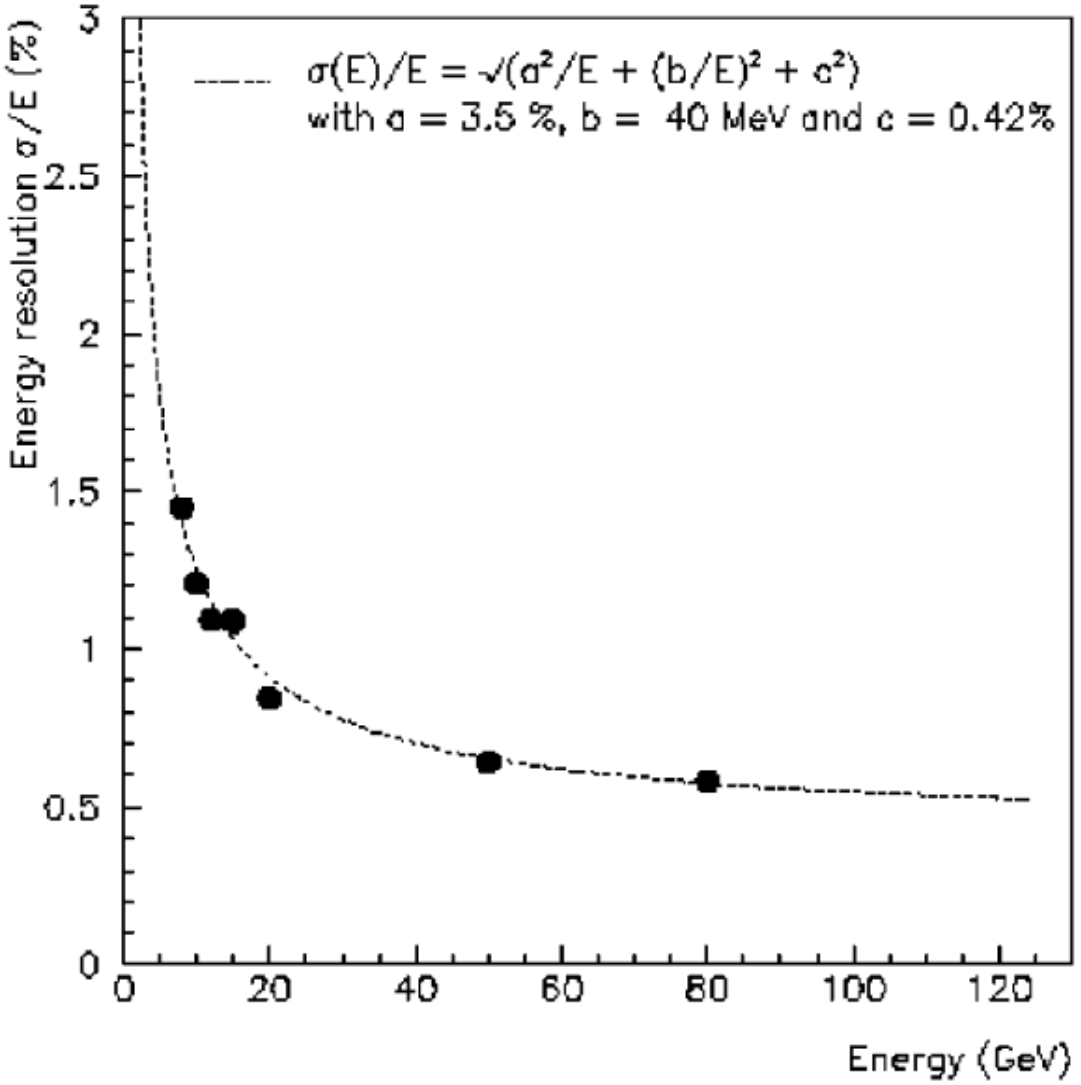

Energieauflösung in OPAL

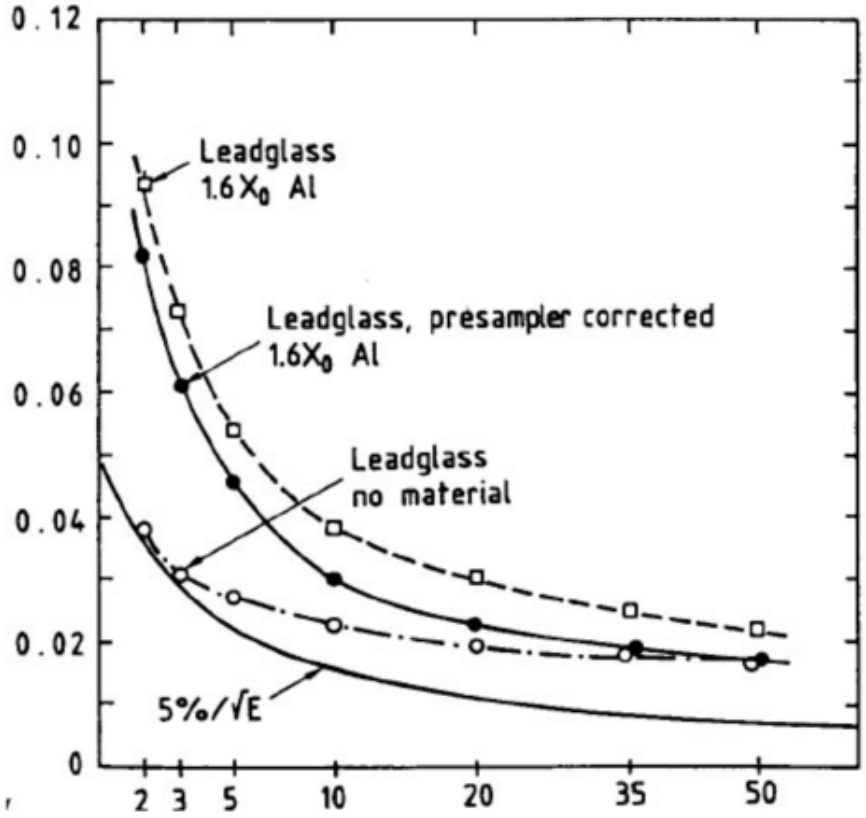

OPAL collaboration, C. Beard et al. NIM A 286 (1990) 117.

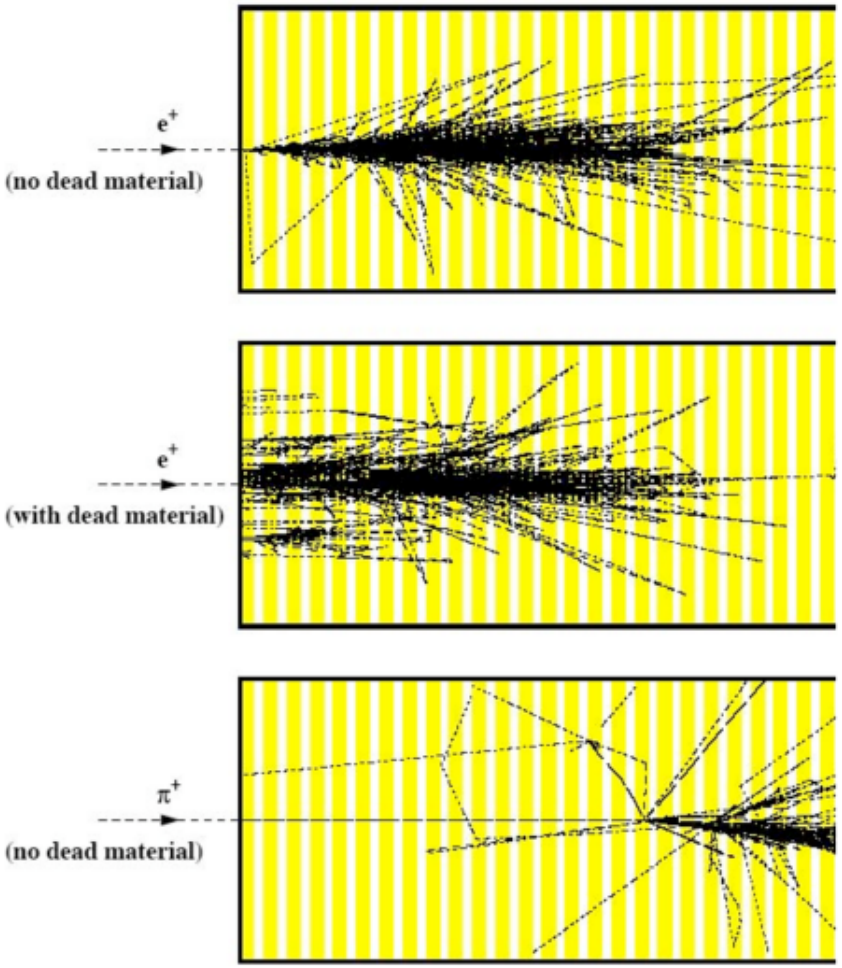

Materialcharakteristika für Kristallkalorimeter

TABLE I. Main properties of crystals commonly used for homogeneous electromagnetic calorimeters in accelerator experiments.

	NaI(Tl)	CsI(Tl)	CsI	BGO	$PbWO_4$
Density (g/cm^3)	3.67	4.53	4.53	7.13	8.28
X_0 (cm)	2.59	1.85	1.85	1.12	0.89
R_M (cm)	4.5	3.8	3.8	2.4	2.2
Decay time (ns)	250	1000	10	300	5
slow component			36		15
Emission peak (nm)	410	565	305	410	440
slow component			480		
Light yield γ/MeV	4×10^4	5×10^4	4×10^4	8×10^3	1.5×10^2
Photoelectron yield (relative to NaI)	1	0.4	0.1	0.15	0.01
Rad. hardness (Gy)	1	10	10^3	1	10^5

Materialcharakteristika für Flüssigedelgaskalo.

TABLE II. Main properties of liquid argon, krypton, and xenon.

	Ar	Kr	Xe
Z	18	36	58
A	40	84	131
X_0 (cm)	14	4.7	2.8
R_M (cm)	7.2	4.7	4.2
Density (g/cm^3)	1.4	2.5	3.0
Ionization energy (eV/pair)	23.3	20.5	15.6
Critical energy ϵ (MeV)	41.7	21.5	14.5
Drift velocity at saturation (mm/μs)	10	5	3

Auslesemöglichkeiten für Sampling-Kalorimeter

Beispiele für Aufbau und Auslese von Sampling-Kalorimeter

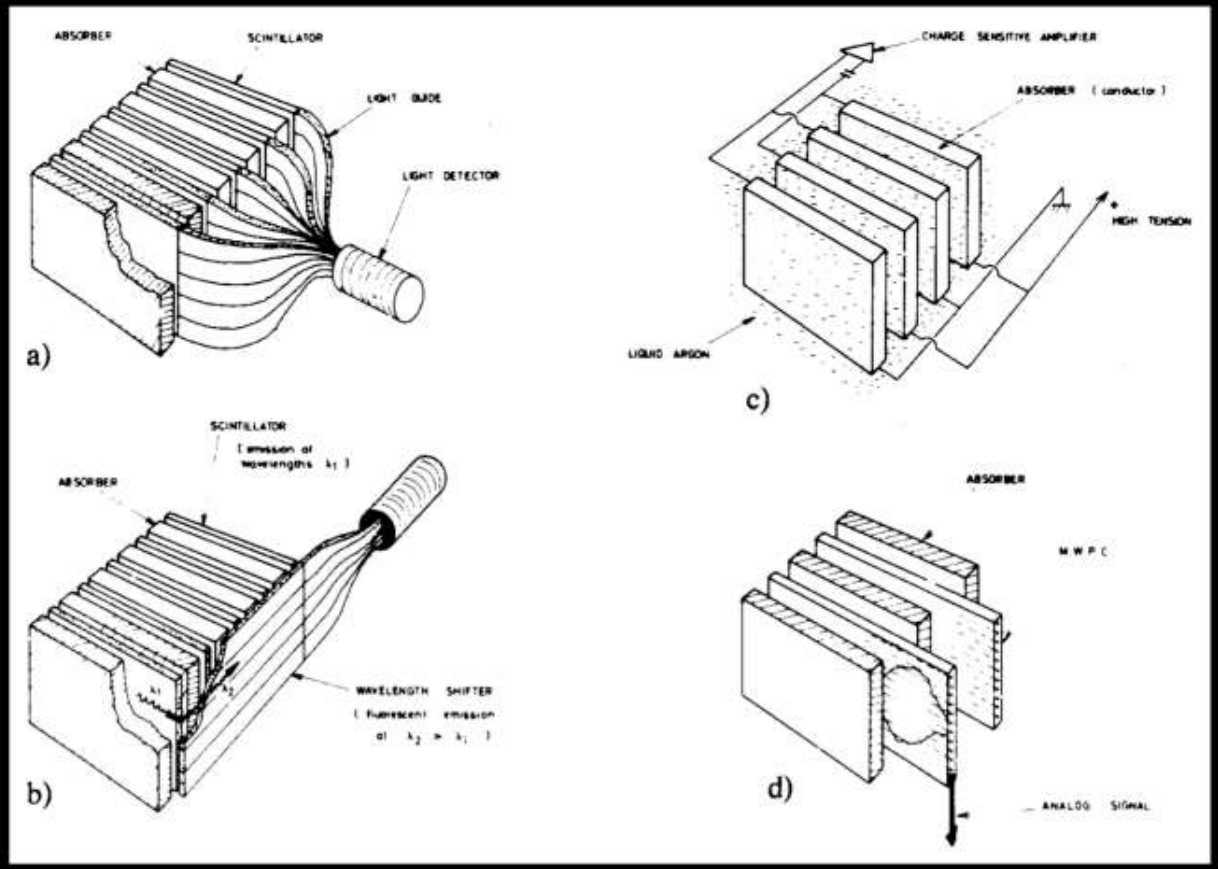

Geometrien der Auslese

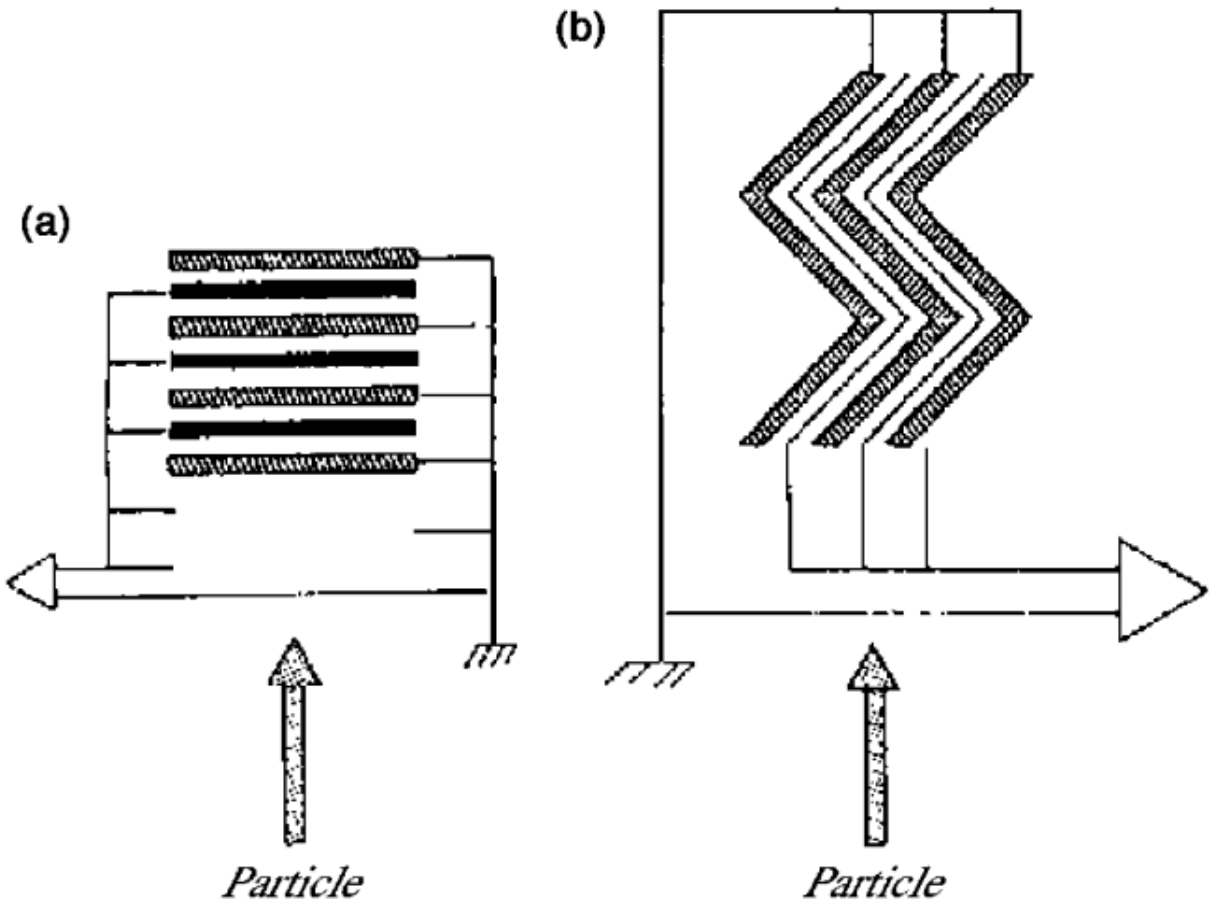

FIG. 15. Schematic view of a traditional sampling calorimeter geometry (a) and of the accordion calorimeter geometry (b).

Energieauflösungen: Beispiele

Technology (Experiment)	Depth	Energy resolution	Date
NaI(Tl) (Crystal Ball)	$20X_0$	$2.7\%/\mathrm{E}^{1/4}$	1983
$Bi_4Ge_3O_{12}$ (BGO) (L3)	$22X_0$	$2\%/\sqrt{E} \oplus 0.7\%$	1993
CsI (KTeV)	$27X_0$	$2\%/\sqrt{E} \oplus 0.45\%$	1996
CsI(Tl) (BaBar)	16–$18X_0$	$2.3\%/E^{1/4} \oplus 1.4\%$	1999
CsI(Tl) (BELLE)	$16X_0$	1.7% for $E_\gamma > 3.5$ GeV	1998
$PbWO_4$ (PWO) (CMS)	$25X_0$	$3\%/\sqrt{E} \oplus 0.5\% \oplus 0.2/E$	1997
Lead glass (OPAL)	$20.5X_0$	$5\%/\sqrt{E}$	1990
Liquid Kr (NA48)	$27X_0$	$3.2\%/\sqrt{E} \oplus 0.42\% \oplus 0.09/E$	1998
Scintillator/depleted U (ZEUS)	20–$30X_0$	$18\%/\sqrt{E}$	1988
Scintillator/Pb (CDF)	$18X_0$	$13.5\%/\sqrt{E}$	1988
Scintillator fiber/Pb spaghetti (KLOE)	$15X_0$	$5.7\%/\sqrt{E} \oplus 0.6\%$	1995
Liquid Ar/Pb (NA31)	$27X_0$	$7.5\%/\sqrt{E} \oplus 0.5\% \oplus 0.1/E$	1988
Liquid Ar/Pb (SLD)	$21X_0$	$8\%/\sqrt{E}$	1993
Liquid Ar/Pb (H1)	20–$30X_0$	$12\%/\sqrt{E} \oplus 1\%$	1998
Liquid Ar/depl. U (DØ)	$20.5X_0$	$16\%/\sqrt{E} \oplus 0.3\% \oplus 0.3/E$	1993
Liquid Ar/Pb accordion (ATLAS)	$25X_0$	$10\%/\sqrt{E} \oplus 0.4\% \oplus 0.3/E$	1996

OPAL-Bleiglaskalorimeter

- Layout

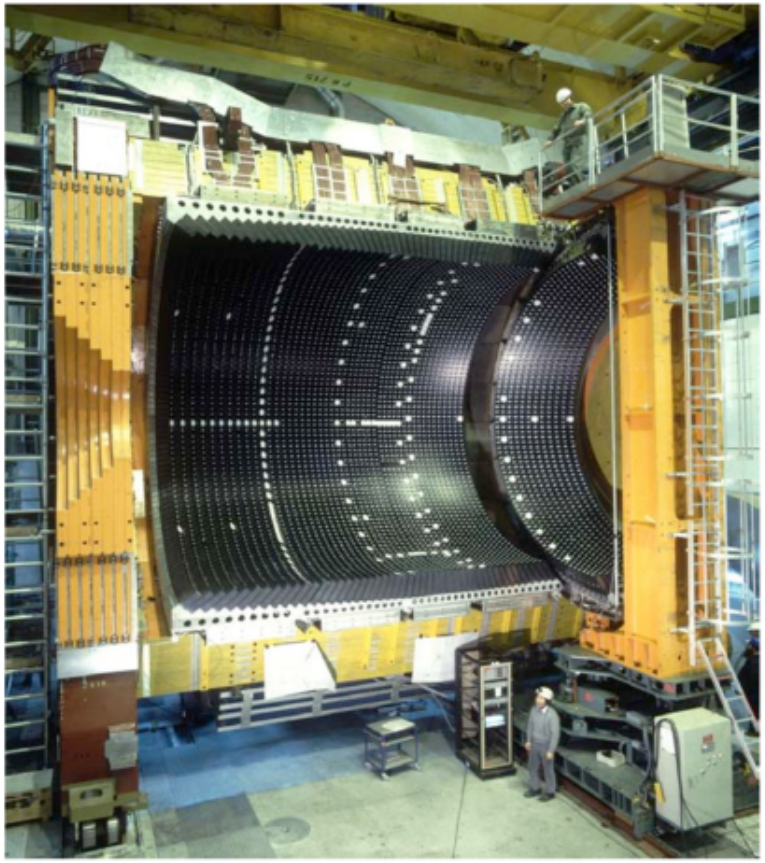

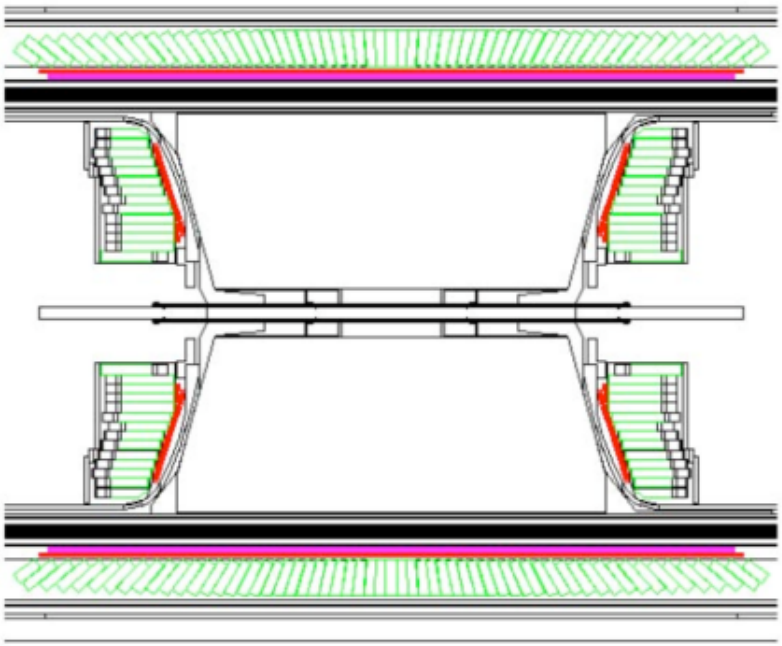

OPAL collaboration, C. Beard et al. NIM A 305 (1991) 275.

- 10572 Pb-glass blocks ($24.6X_0$)
- Energy resolution: $\frac{\sigma_E}{E} = \frac{6\%}{\sqrt{E}} \oplus 0.002$
- Spatial resolution: 11mm at 6GeV

Zwei-Photon-Ereignisse in der Higgs-Suche

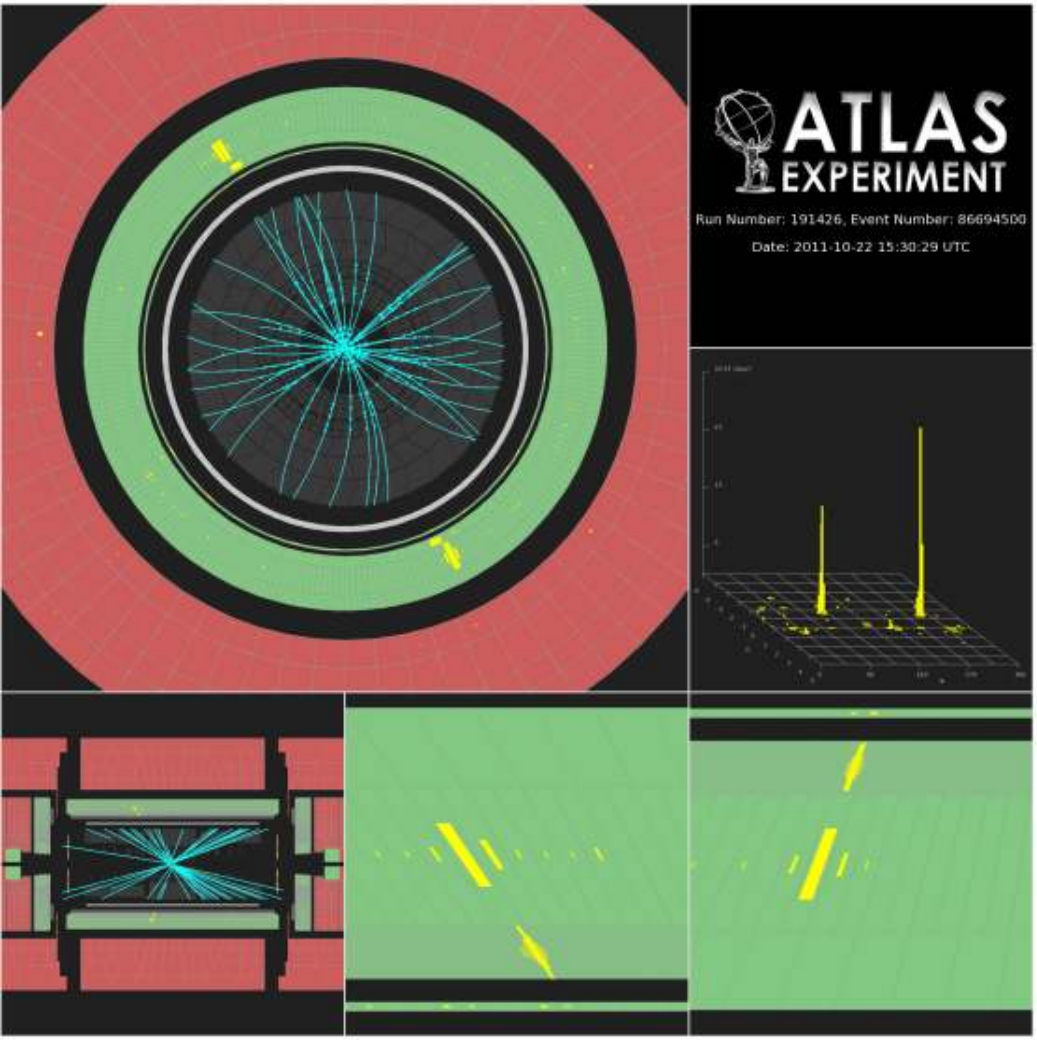

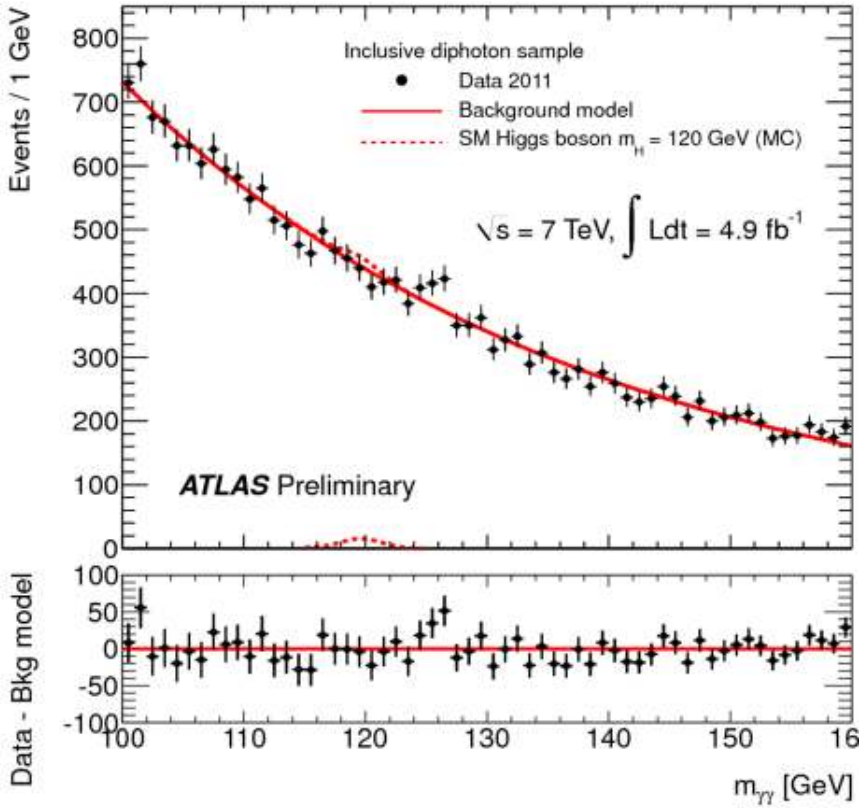

Ein W→Elektron+Neutrino Ereignis bei ATLAS

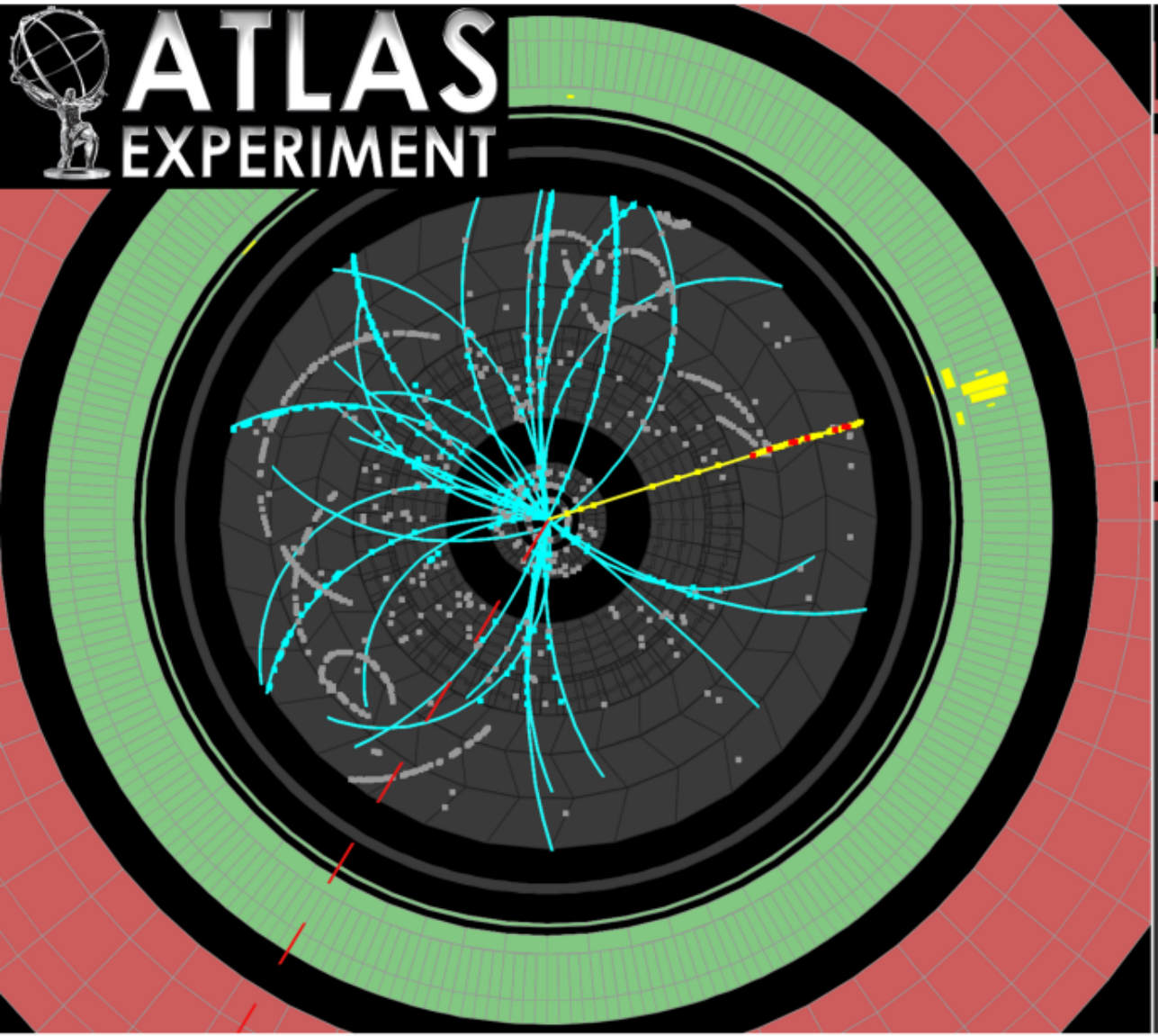

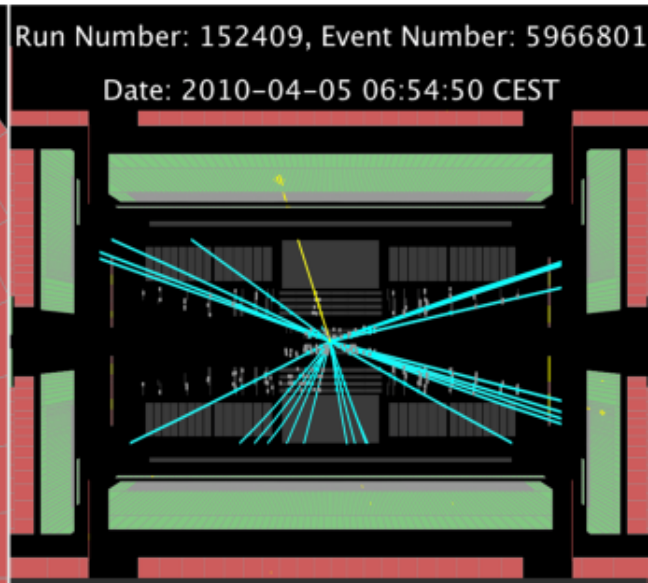

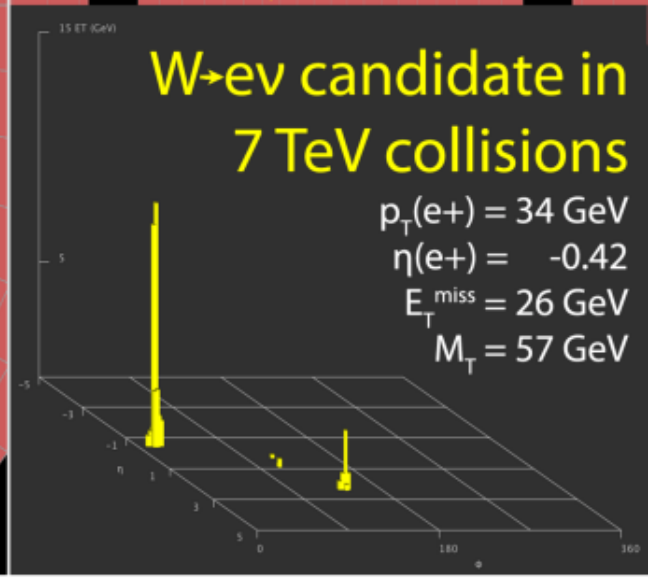

Eine Ereignis in der Suche nach Supersymmetrie

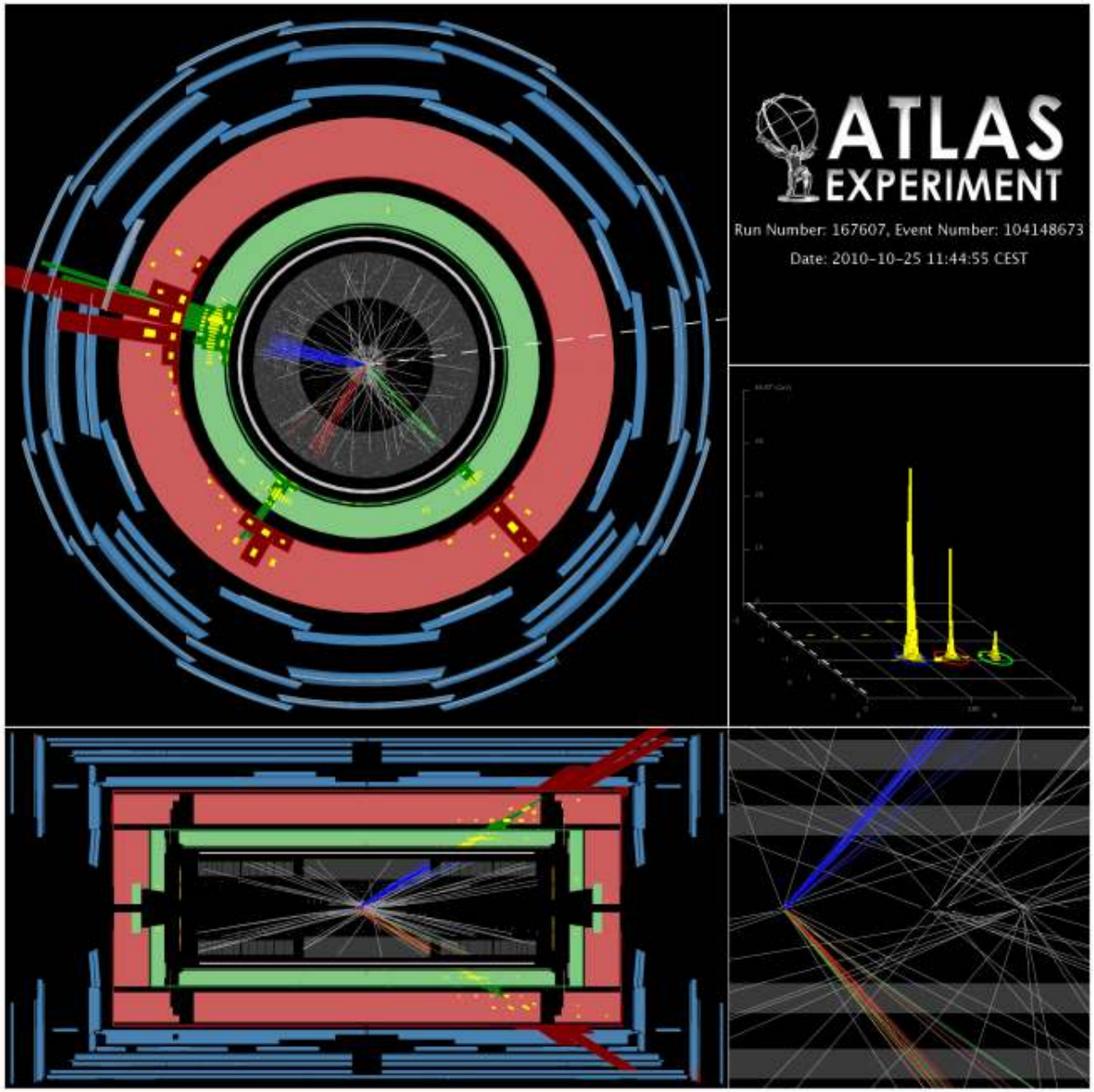

Unterscheidung von WW/ZZ→ 4 jets am ILC

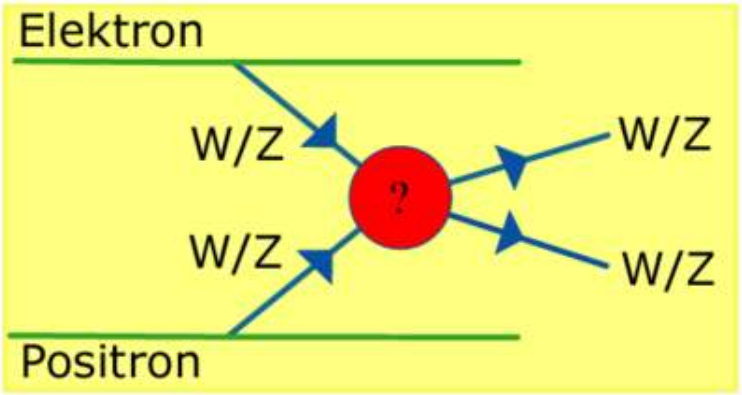

Bestimmung der beiden Dijetmassen: Unterscheidung WW und ZZ

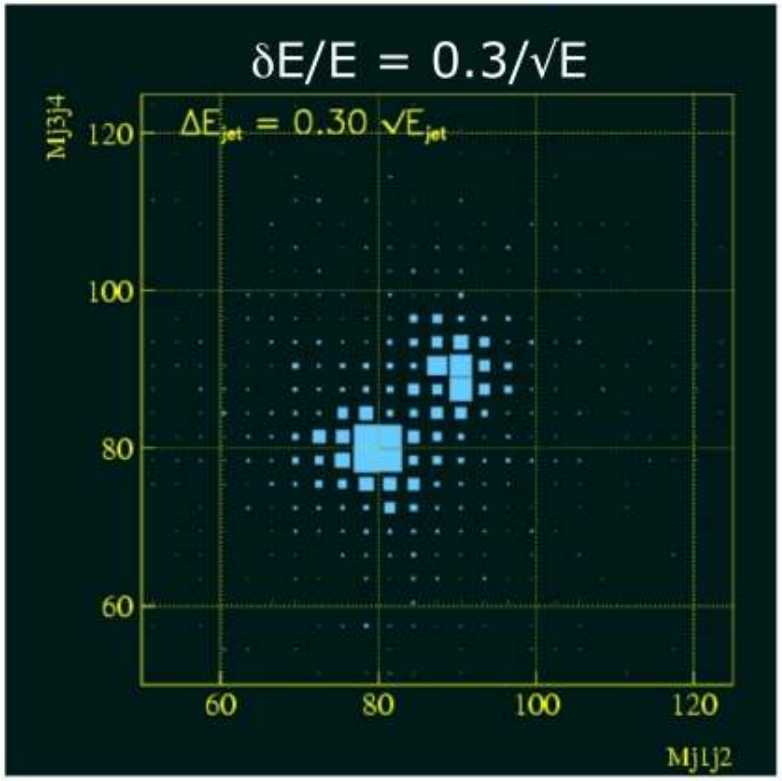

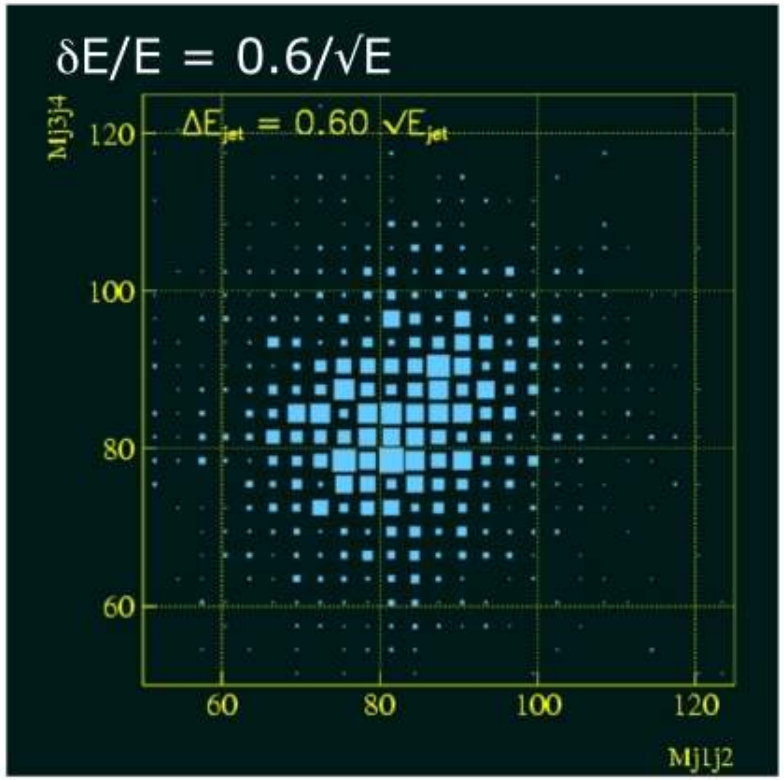

Hadronischer Schauer

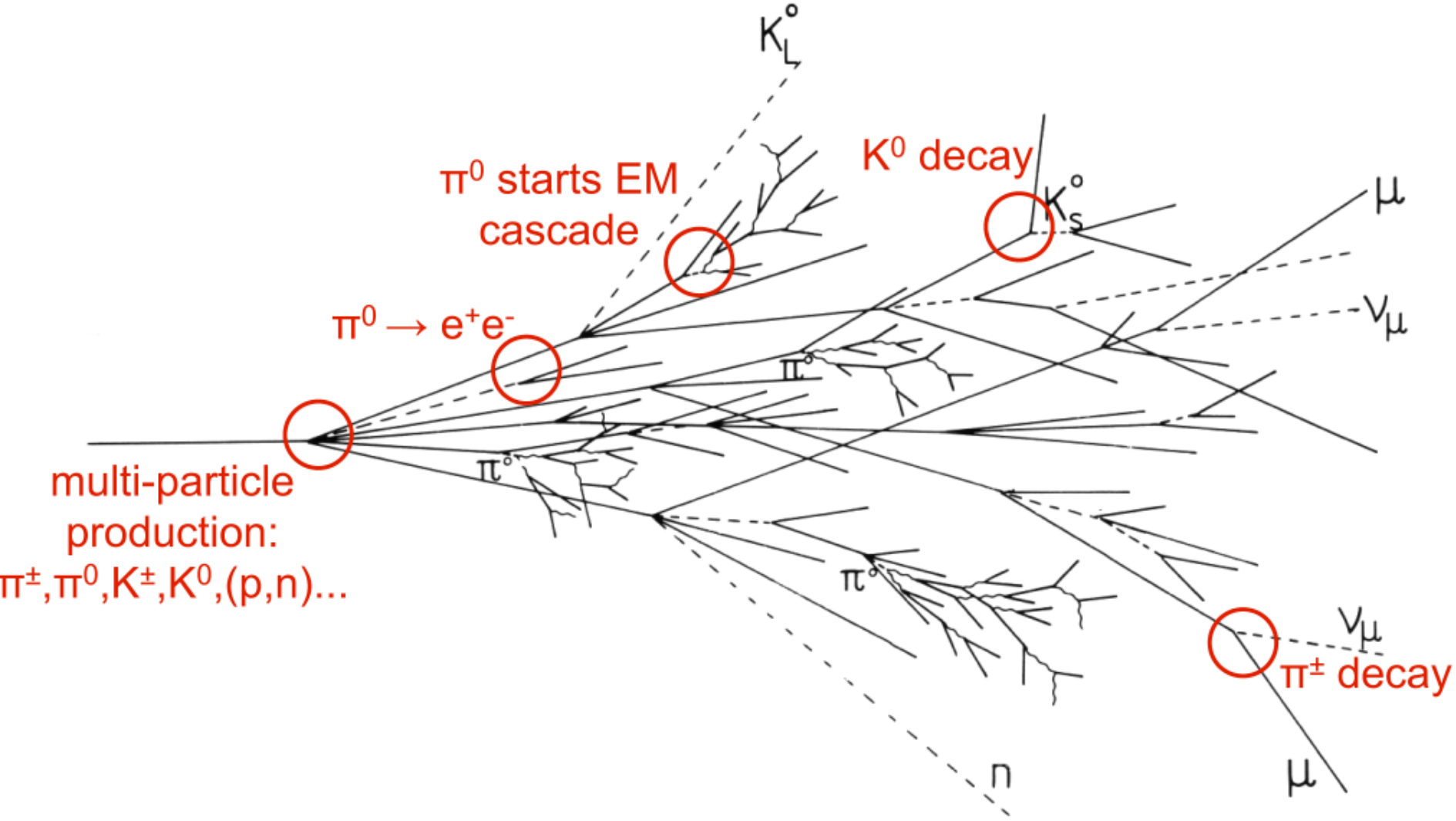

Fig. 7.32. Sketch of a hadron cascade in an absorber.

Hadronischer Schauer

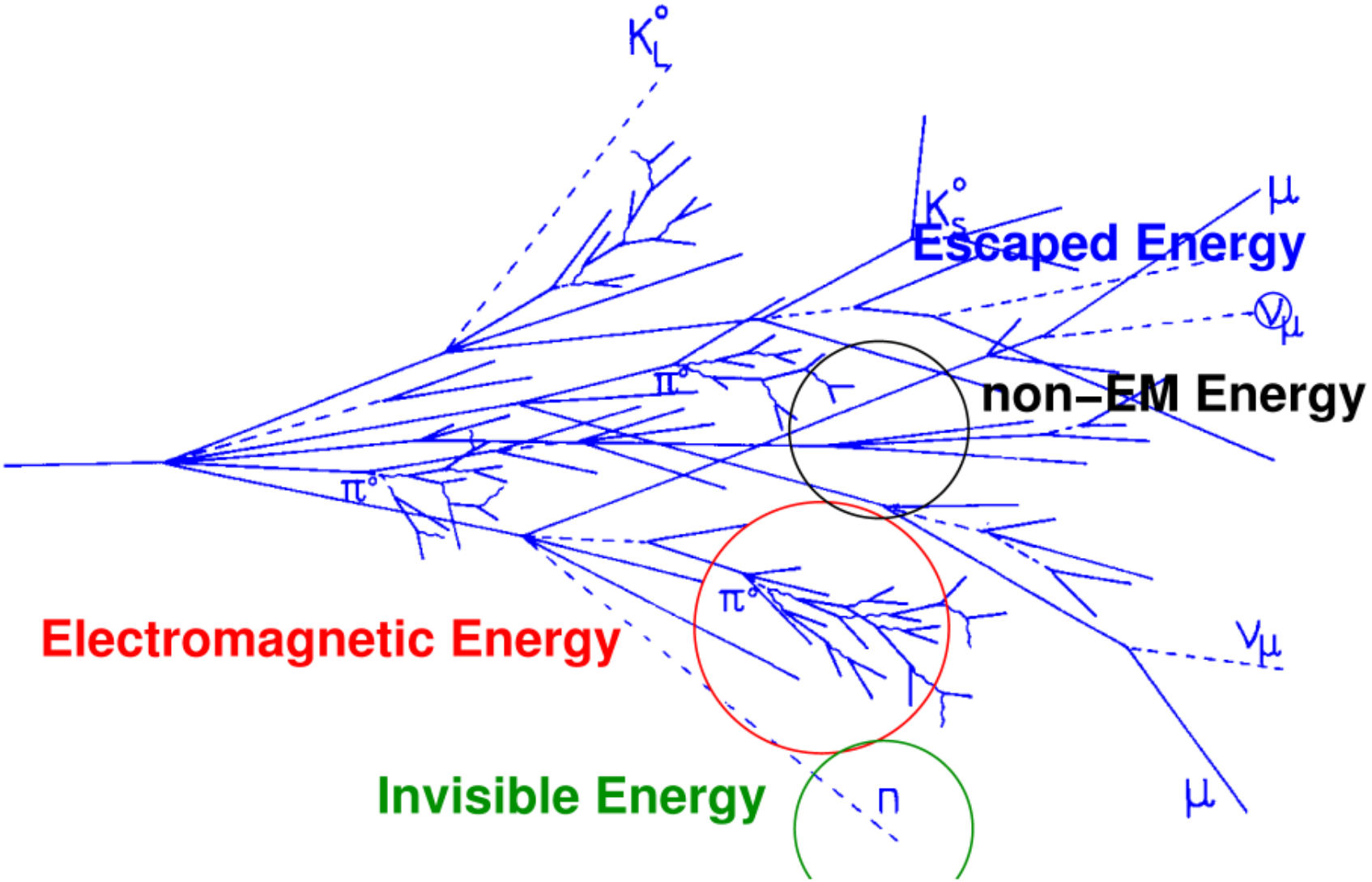

Hadronic and e.m. showers:

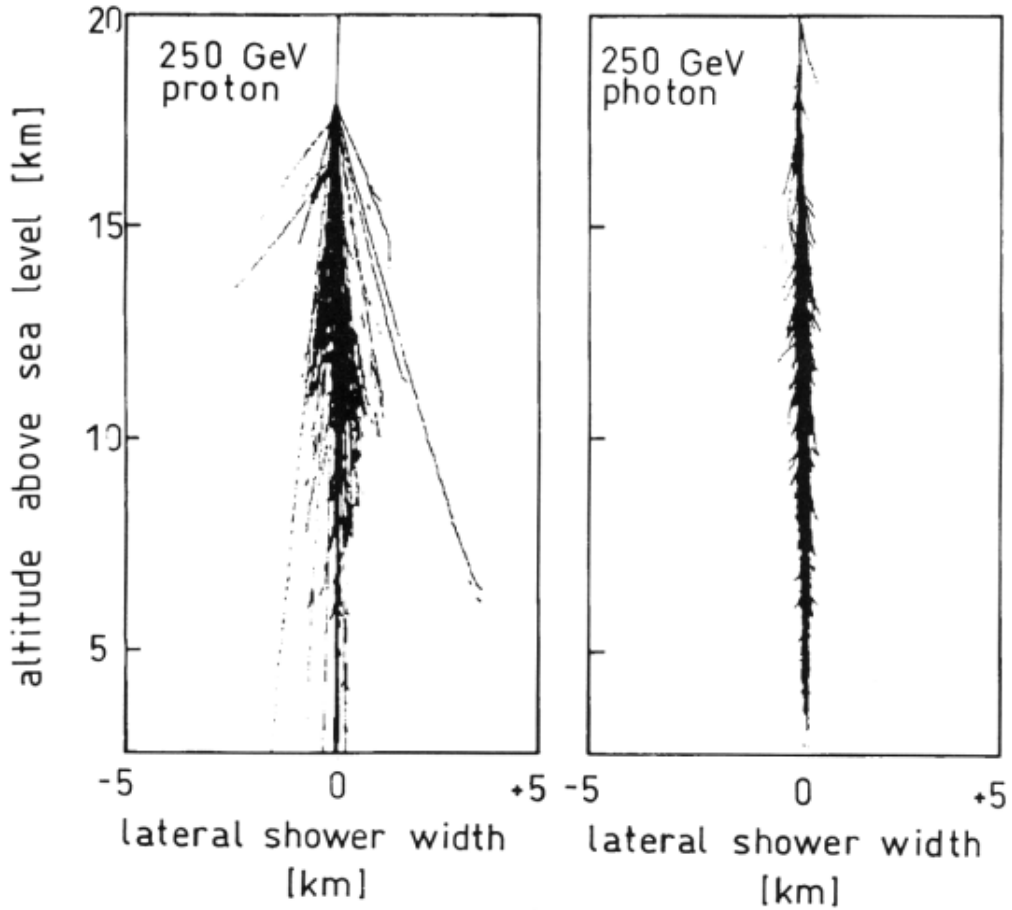

Fig. 7.34. Monte Carlo simulations of the different development of hadronic and electromagnetic cascades in the earth's atmosphere, induced by 250 GeV protons and photons [542].

Differences:

- Hadronic showers are much wider than electromagnetic ones (*Reason: angle of particle emission is determined by intrinsic transverse momenta of quarks, $p_T \approx 0.35$ GeV/c*)
- Hadronic showers are more irregular than electromagnetic ones (*Reasons: multiplicity of produced hadrons varies considerably around average; decay of unstable particles)*
- Energy resolution of hadronic showers is worse (*Reasons: stronger fluctuations, decays produce neutrinos that carry away some energy)*

Hadronischer Schauer

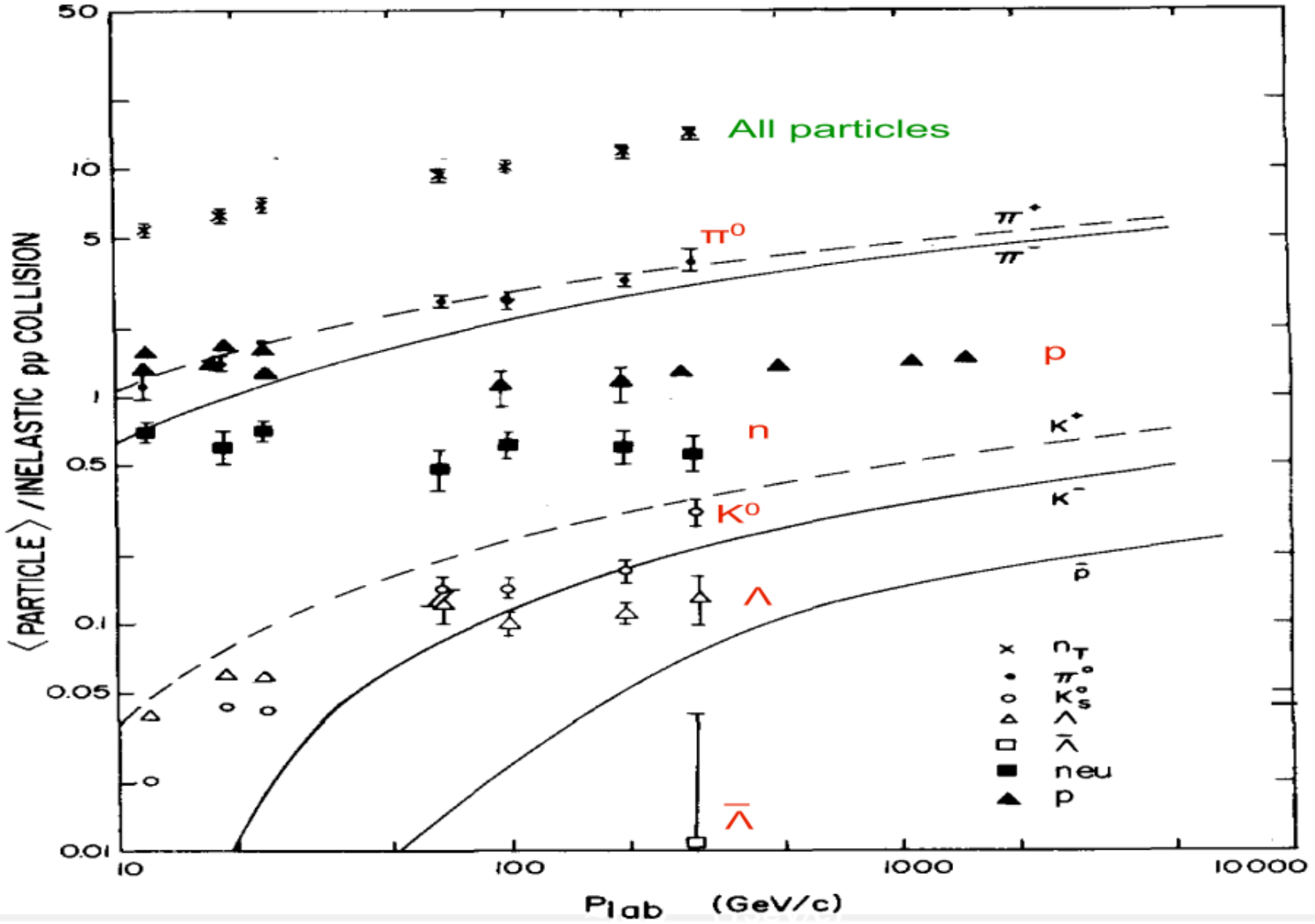

Prozesse im hadronischen Schauer

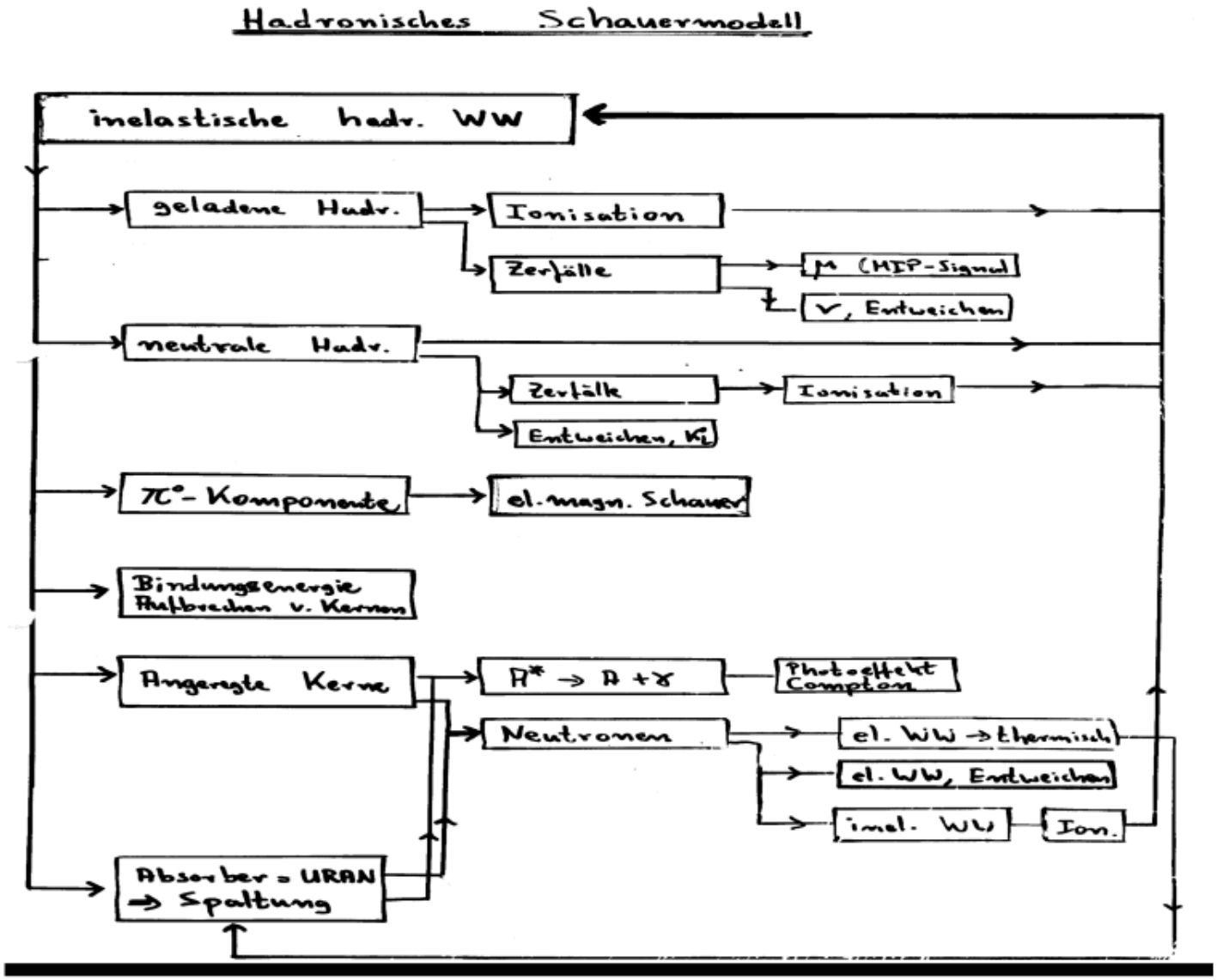

Energieanteile in hadronischen Schauern

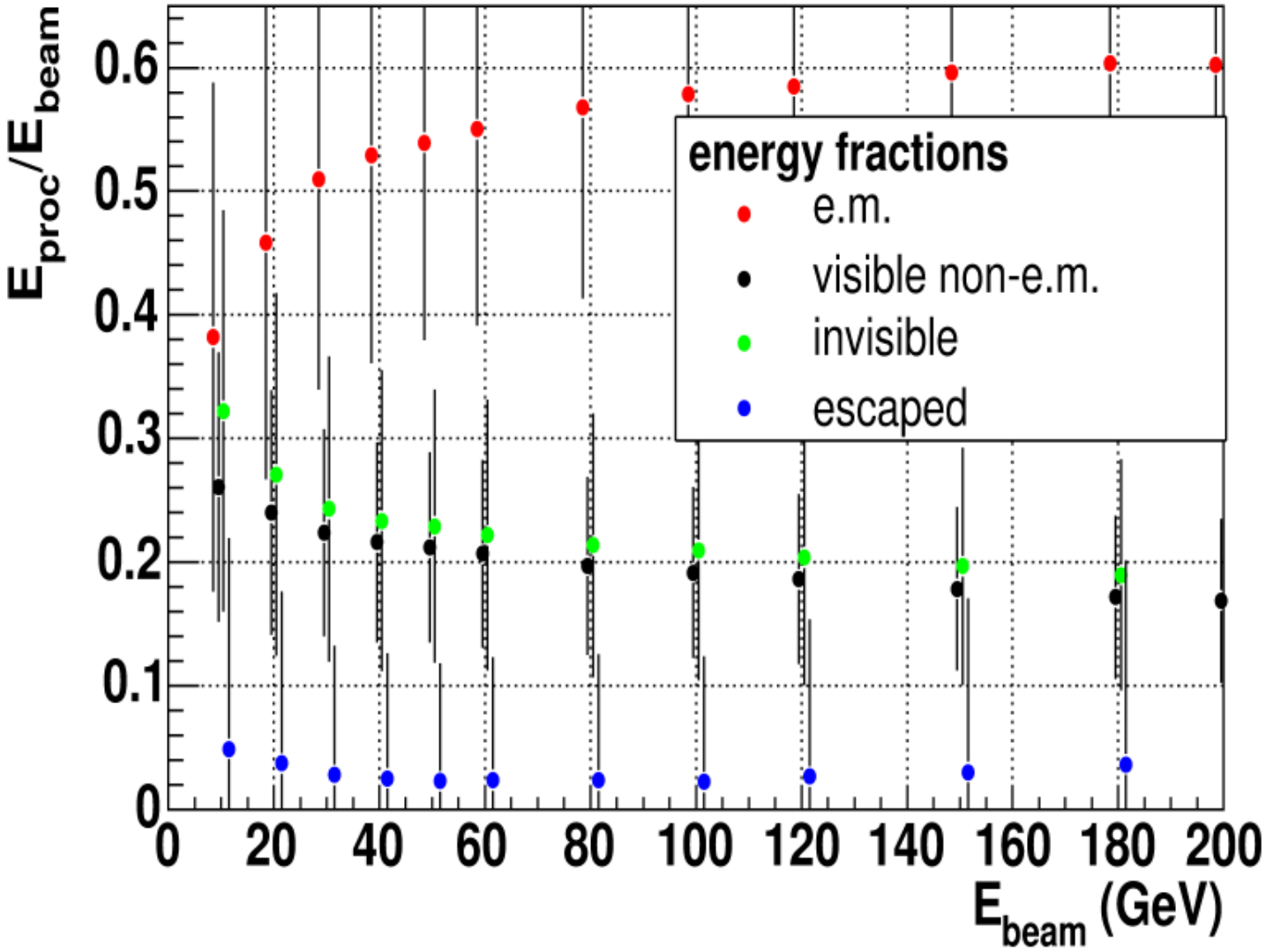

hadronische Wechselwirkungslänge

Material	Z	A	Z/A	X_0 (cm)	λ_I (cm)	Density (g/cm^3)
H_2 (liquid)	1	1.008	0.992	866	718	0.0708
He	2	4.002	0.500	756	520	0.125
C	6	12.01	0.500	18.8	38.1	2.27
Al	13	26.98	0.482	8.9	39.4	2.70
Cu	29	63.55	0.456	1.43	15.1	8.96
Pb	82	207.2	0.396	0.56	17.1	11.4
W	74	183.8	0.403	0.35	9.58	19.3
U	92	238.0	0.387	0.32	10.5	19.0
Scint.			0.538	42.4	81.5	1.03
BGO			0.421	1.12	22.1	7.10
CsI			0.416	1.85	36.9	4.53
NaI			0.427	2.59	41.1	3.67

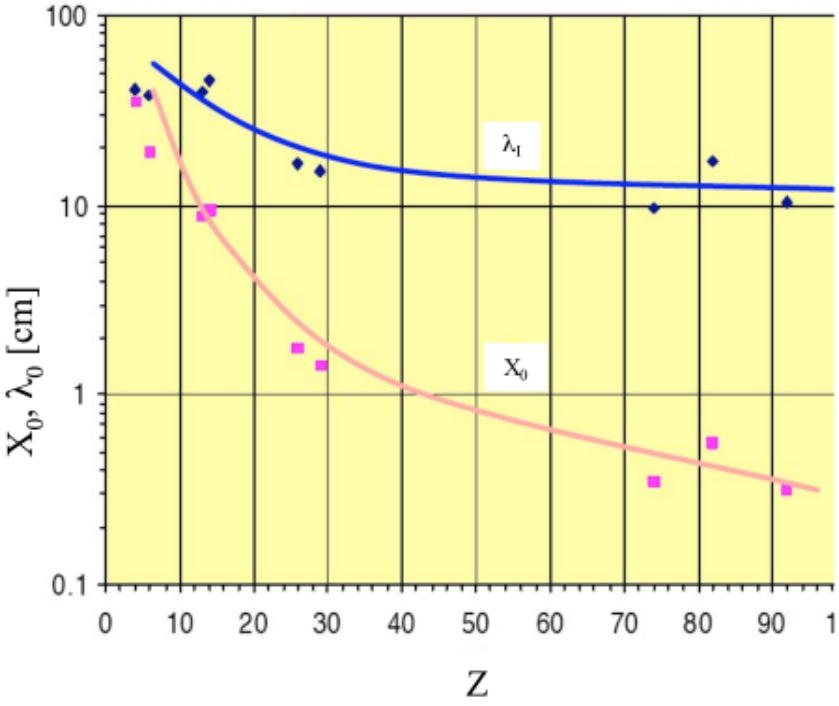

Hadronic shower profiles; radial distribution:

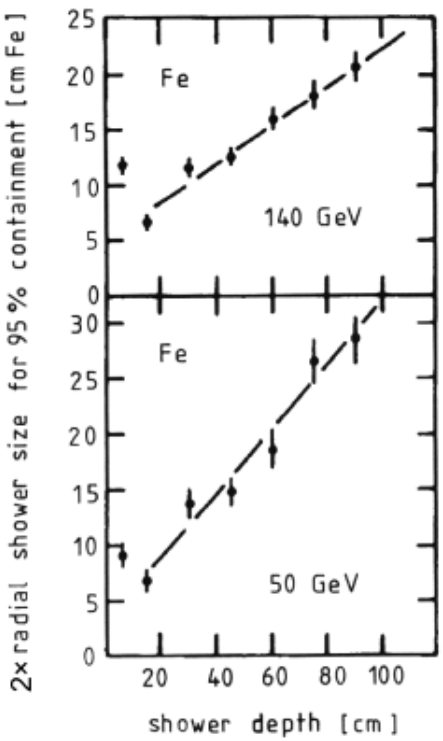

7.43. Radius of hadronic showers for 95 % containment as a function of depth in iron [555]. The corresponding total width of the hadron shower is ce the radius.

- Radial size increases linearly with shower depth
- Maximum radius approx. independent of incident energy
- $R(95\%) \approx \lambda_I$

Example: pions on iron, λ_I = 16.7 cm
R(95%) = 16.7 cm
approx. for all energies!

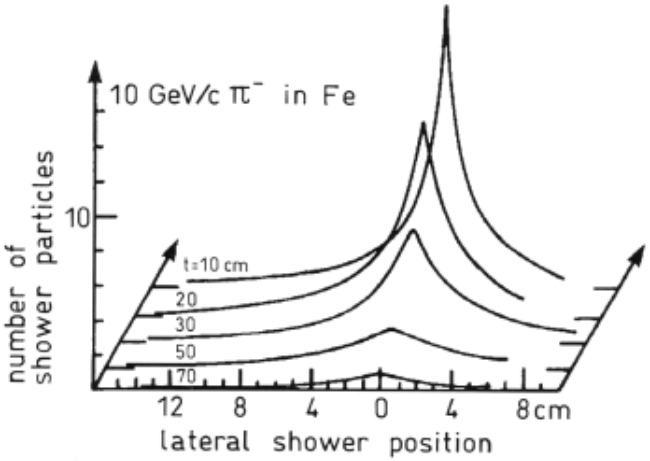

Fig. 7.39. Lateral shower profile of 10 GeV/c pions in iron [559].

Hadronic shower profiles; electromagnetic content:

f_{em} : electromagnetic fraction of shower

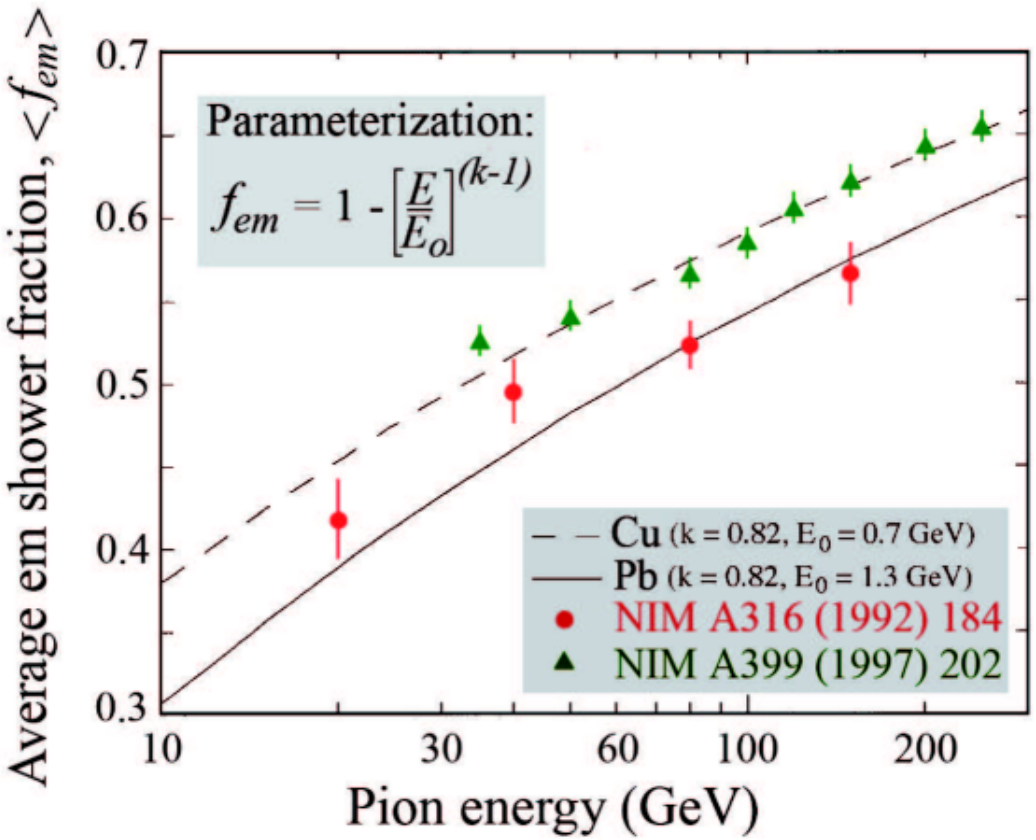

f_{em}:

- depends on energy of incident particle
- depends (weakly) on target material
- can reach more than 60%!

non-e.m. energy fractions:

- 56% ionizing particles (from which 2/3 protons!)
- 10% neutrons
- 34% invisible energy

Fluktuationen im hadronischen Schauer

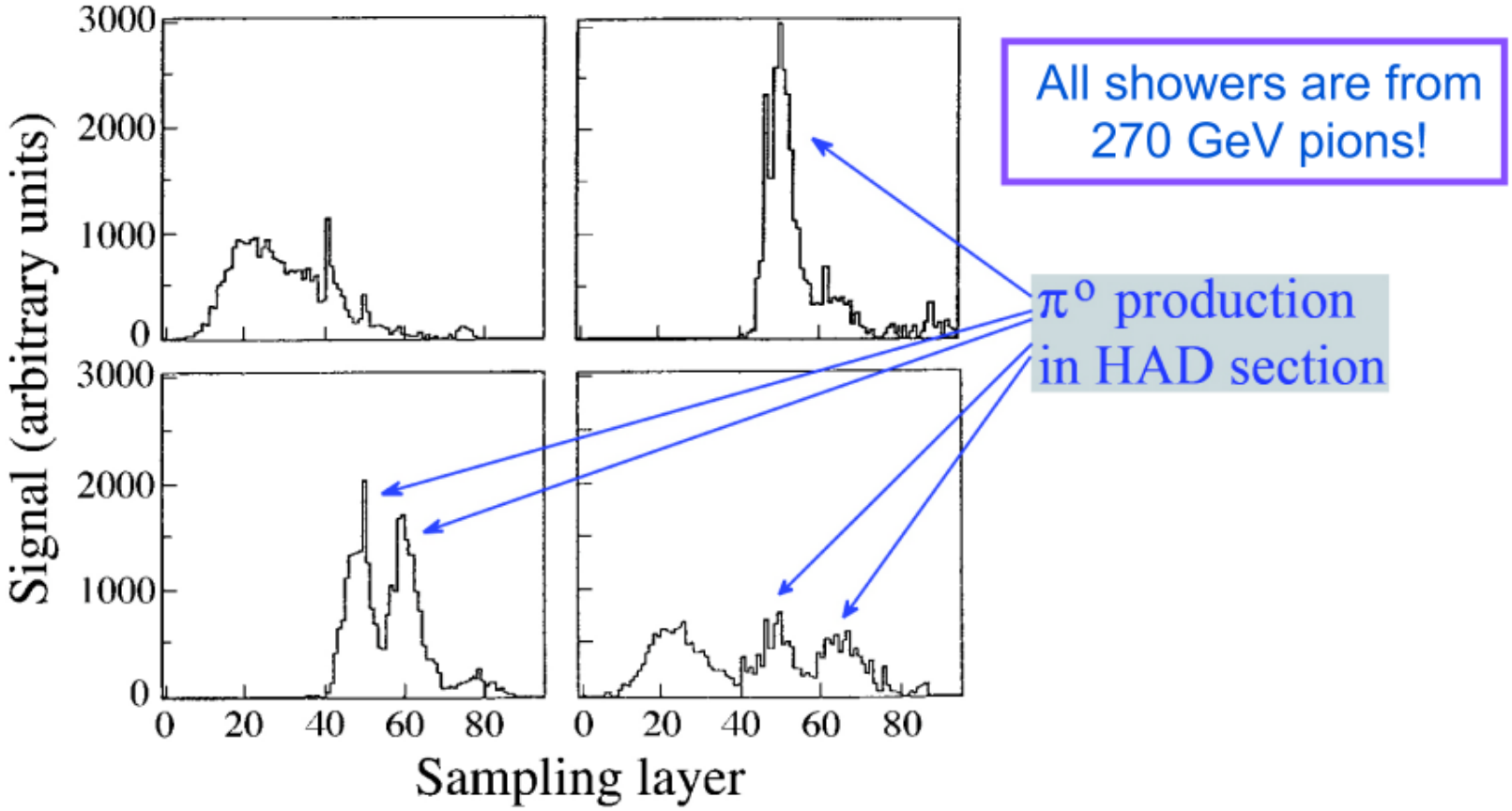

Fig. 7: Longitudinal profiles for 4 different showers induced by 270 GeV pions in a lead/iron/plastic-scintillat calorimeter [5].

Detektorantwort als Funtion von e/h

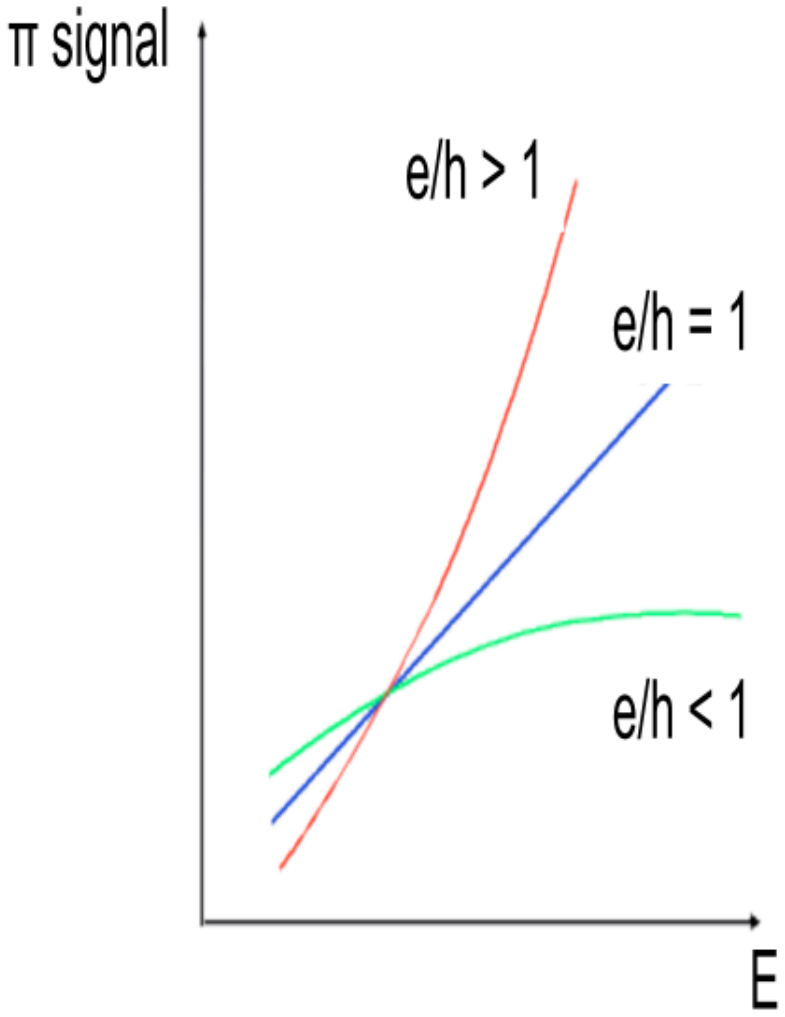

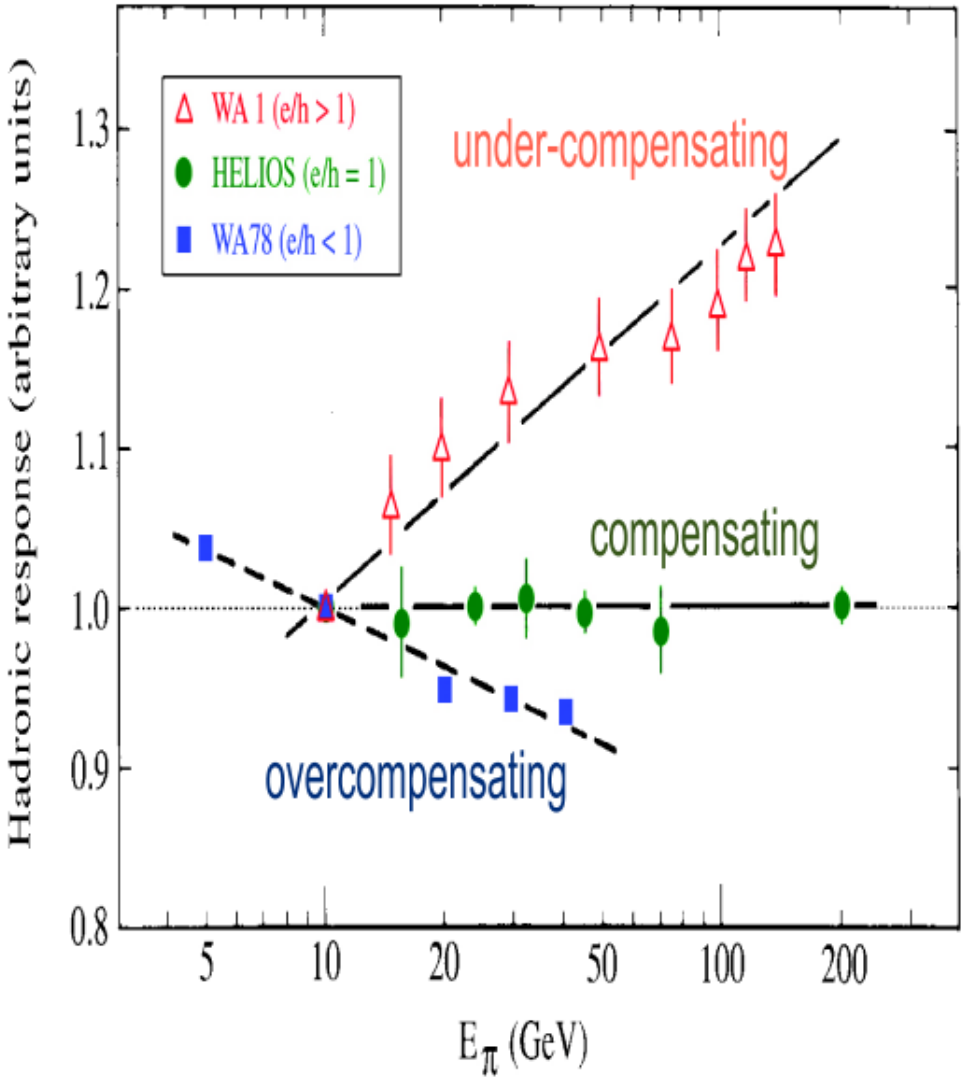

Compensating calorimeters (cntd):

Compensation is *only* possible in *sampling* calorimeters!

3 Methods to achieve compensation (e/h = 1) :

1. **Reduce** response to **e.m. component**
   - Choose high-Z absorber (e.g. Pb, U) and low-Z active medium
   - photoelectron production $\propto Z^5 \Rightarrow$ most photoelectrons are produced and absorbed in Pb
     few photoelectrons are produced in active medium
2. **Enhance** response to **hadronic component**
   - use slow neutrons to induce nuclear fission, e.g. in ^{238}U
   - additional neutrons are produced
   - the neutrons escape into the active medium (low A)
   - the neutrons are slowed down via elastic n-p-collisions
   - the protons produce a signal in the detection medium
3. **Offline compensation**
   - Disentangle contributions from hadronic and electromagnetic showers from the spacial development in high resolution calorimeters

   OR:
   - compare fraction of szintillator and Čerenkov light (e.m. processes create relativistic electrons (Čerenkov light), spallation protons from nuclear fission and recoil protons from the n-p scattering in the detection medium are non-relativistic)

Energieauflösung und Linearität in Abh. von e/h

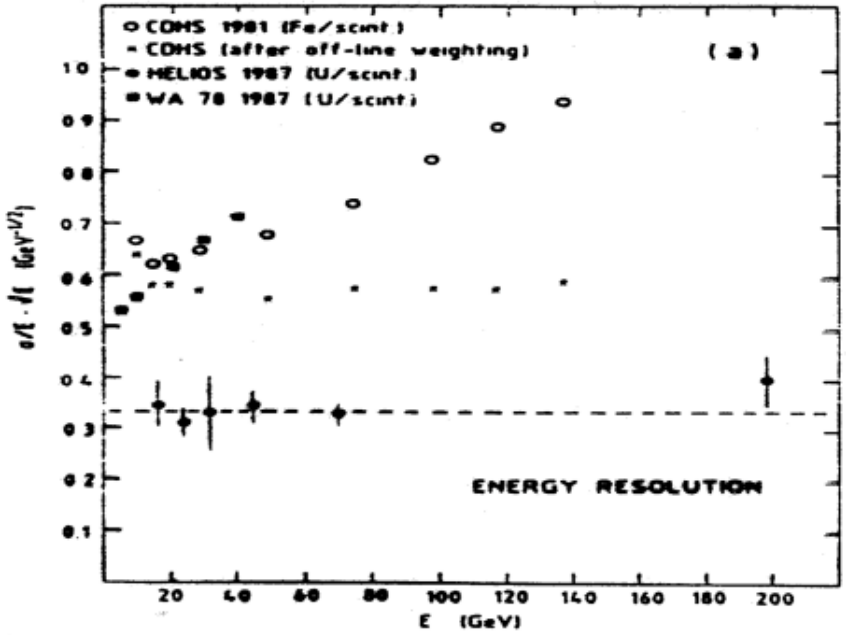

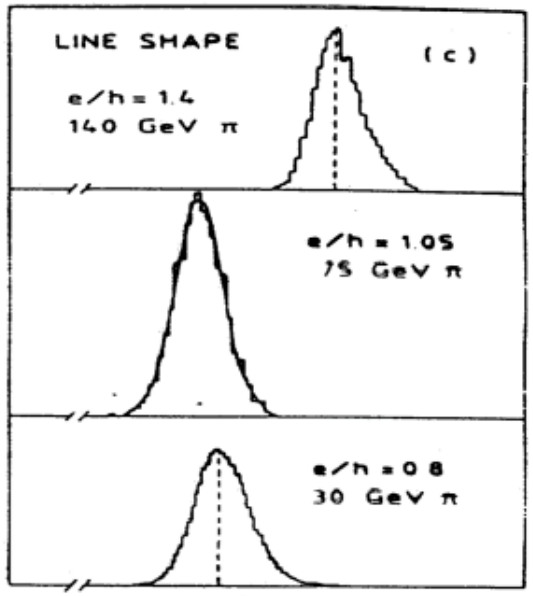

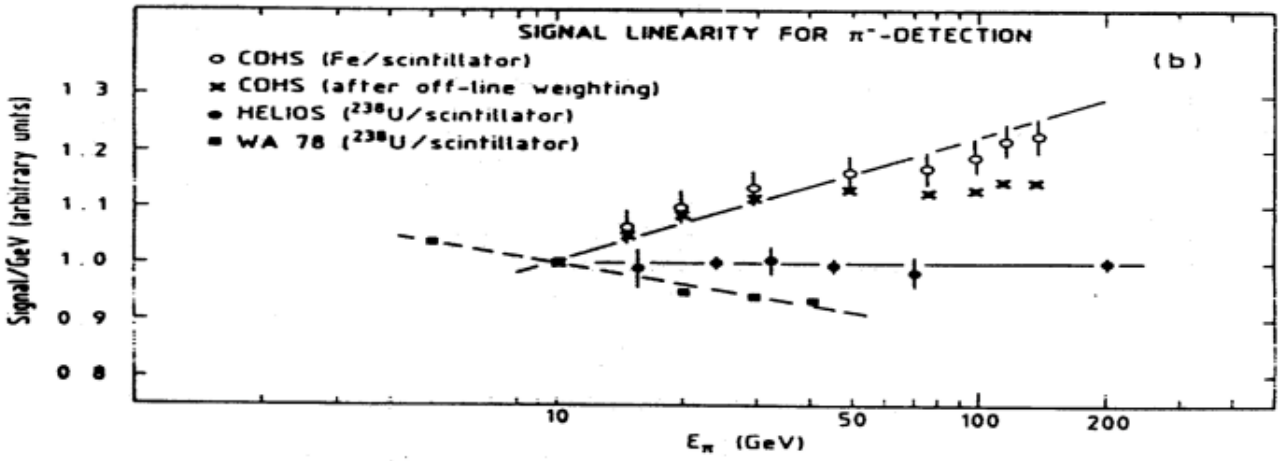

Kompensation in Pb-Kalorimeterrn

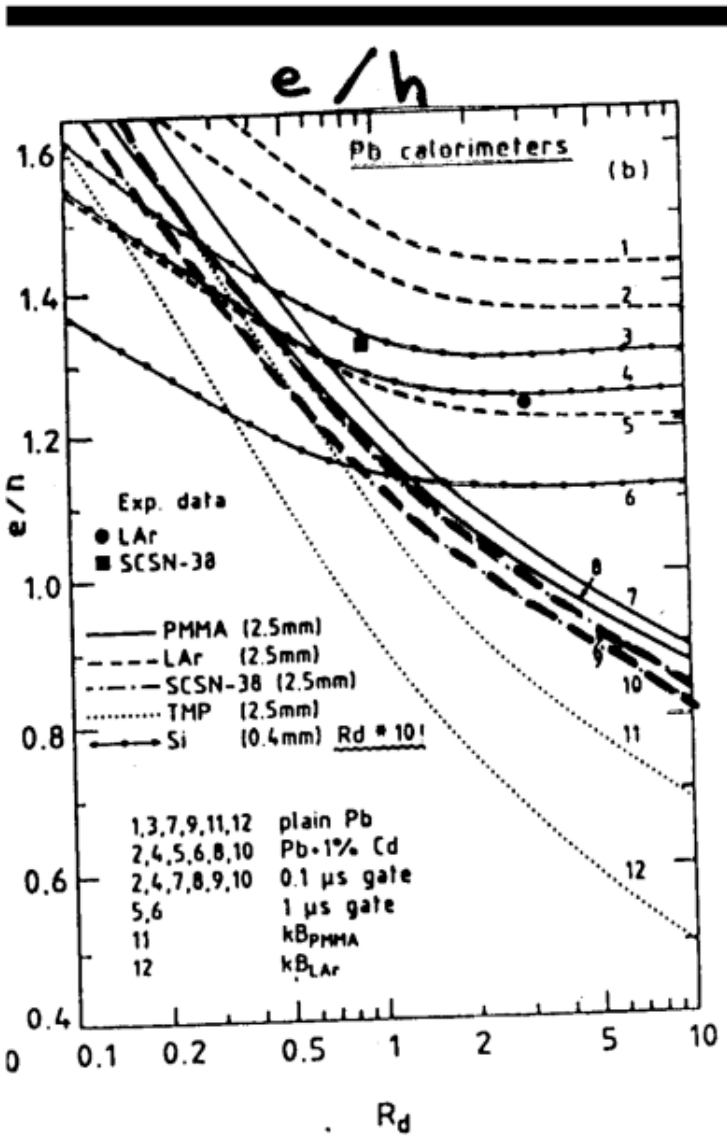

Blei-Kalorimeter

LAr

-- Szintillator

$$R_d = \frac{t_{obs.}}{t_{akt.}}$$